PENNSTATE

June 28, 2009

Prof. Jan Seibert

Dear Jan,

Enclosed here please find the revised manuscript, entitled "***Simulation and Validation of Concentrated Subsurface Lateral Flow Paths in an Agricultural Landscape***" that was submitted to *HESS* special issue "The Earth's Critical Zone and Hydropedology" (***hess-2009-71***). We have now completed a careful revision according to all the review comments received. We appreciate the time the reviewers and you put in reading the manuscript, and the comments were valuable, refreshing, and constructive. A list of itemized responses to all review comments is attached at the end of this letter, along with a tracked-change copy of the revised manuscript. I hope we have adequately addressed all the review comments to your satisfaction. Should you have any questions or need further information or action from me, please let me know.

Thanks for your further consideration of this manuscript.

Sincerely Yours,

Henry Lin
Associate Professor of Hydropedology/Soil Hydrology

Encl.: 1) Revised manuscript (clean copy)
2) Item-by-item responses to all the review comments, plus an annotated version of the revised manuscript (changes marked using Word "Track change" function)

Item-by-item responses to all review comments

NOTE: To facilitate the evaluation of our responses, original review comments are listed first in their originals (in black), followed by our itemized responses **(in red, italic and bold)**. An annotated version of the revised manuscript is also enclosed.

Comments from the editor

1. I would suggest changing the word verification to validation (or testing) in the title (and text). In my PhD Thesis I discussed these terms a bit (see p. 16f in my thesis which you can download from http://people.su.se/~jseib/publications.htm (scroll to the end))

Thanks for catching this. We have changed this as suggested before publishing in HESSD.

2. Explain (or replace) Ap1 and Ap2 in the abstract (and text).

We have changed this as suggested before publishing in HESSD.

3. I am very much in favor of separating results and discussion and think this would make the the paper easier to read. However, I leave this decision to you.

We have changed this as suggested. See the new Discussion session in the revised manuscript.

Reviewer 1

General comments

This is an interesting manuscript with focus on identification of subsurface lateral flow paths in agricultural landscapes. Three different validation methods were used to evaluate the results of flow pathways calculations. Detailed soil and field surveys are the strengths of this study. I suggest publishing this manuscript with consideration taken to comments below.

Thanks for the encouraging comments.

Specific comments

However I feel that the manuscript can be improved if following comments are taken into consideration:

1. Authors state that “the topography of the three interfaces was dominated by the variation in land surface elevation, resulting in nearly identical spatial patterns in the simulated lateral flow paths among the three interfaces. “(page 2906, line 4-7). I found it then difficult to understand why the land surface elevation itself was not used as one interface to simulate subsurface flow paths, at least to study to what degree the other interfaces improve these calculations. So I would suggest including this “control” interface.

In our study area and at the farm scale, the simulated flow paths at these three interfaces were quite similar (>98% matched) since the topography of the three interfaces follows that of the surface topography. Besides, in our study area, the maximum difference in surface elevation was 23 m while the largest difference in the Ap1 horizon thickness and depths to the clay layer and the bedrock for the entire landscape were less than 2 m (i.e., < 8.7% of the surface elevation change). Consequently, the topography of the three interfaces was dominated by the variation in land surface elevation, resulting in similar spatial patterns in the simulated lateral flow paths among the three interfaces. We would yield similar results if the surface DEM was used in the simulation.

However, many other studies have found that the DEMs of interfaces were quite different from the surface DEMs. In these cases, the flow path simulations based on the interface DEMs did yield better results than using the surface DEMs (e.g., Freer et al., 2002; Burns et al., 1998). Therefore, we believe that simulation based on the DEM of subsurface interfaces is better off since it would yield results no worse than what would be obtained using surface DEM.

We have now discussed this issue in the new Discussion section, including citations of other relevant studies.

2. I would appreciate some discussion on differences between results received with different interfaces and validation methods, and maybe even suggestions by the authors regarding selection of the appropriate method (interface) and validation technique when scaling-up their results.

This has been added in the new Discussion section. Some suggestions are also provided in the Conclusion section. The added new Table 2 also summarizes some comparisons of validation techniques. However, we were not quite sure what "scaling-up" this reviewer might specifically refer to.

3. The interpolation of point data may influence the final results. Authors write that different methods were used to interpolate different variables (page 2899, lines 6-16), and refer to in-review article (Zhu and Lin, 2009). This leaves small possibilities to evaluate the quality of performed interpolation.

In addition to the article of Zhu and Lin (2009), we also cited other papers (Kravchenko, 2003; Kravchenko and Robertson, 2007) to prove that these soil properties were acceptably interpolated.

4. I would appreciate little more information on chosen validation methods already in the introduction. For instance text on page 2909, from line 23 could be moved to introduction

We have changed this as suggested. The content from line 7 to line 11 on page 2909 was moved into the introduction part to discuss the validation method of EMI. The content from line 23 to line 28 on page 2909 were also moved into the introduction part to discuss the validation method of soil Mn content.

5. Consider omitting Fig 2, it is more or less common knowledge by now and references will be enough.

We have changed this as suggested. However, Figure 2 is not only an illustration of D8 algorithm, but also shows how we determine whether a soil moisture monitoring site is on or off the simulated flow path. Therefore, we deleted the Figure 2 as suggested, but put an illustration of how we determine whether a soil moisture monitoring site is on or off the simulated flow path into the original Figure 3 (now Fig. 2d).

6. Figure 8 may also be omitted, it is not the essential part of the manuscript. It is also referred to in the text before Fig 7.

We have changed this as suggested. Since we deleted some figures as this reviewer suggested, all the figures were re-numbered and organized.

Technical corrections
1. Figure 11. Figure text – what is the last sentence here referring to?

The labels of the bars in the inset graphics of Figure 11 were missed. We revised this figure so the last sentence of the caption "Bars with different letters are statistically significantly different at p<0.05 level" referred to the labels in the inset graphics.

Reviewer 2

General Comments
This is a very nice study that uses GIS to indicate where in a landscape concentrated subsurface flows initiate and travel based on upslope contributing area. The paper is a little cumbersome because of all the variations in approach, consideration of dry and wet periods, and three corroboration methods (also, above vs below discontinuities and on vs off flow paths). Is there a tabular way to summarize all these? Other than that, this paper is publishable with only a few minor changes and perhaps some potential clarifications.

Thanks for the encouraging comments. As this reviewer suggested, a new table (now Table 2) is now added to summarize the algorithm, thresholds, and validation methods used in this study. The old Table 2 was renamed as Table 3 in the revised manuscript.

Specific Comments: (please number lines in the future)
1) Abstract, line 3: specify D8 flow direction

We have changed this as suggested. We specified that the flow direction and accumulation were based on the deterministic 8 method single-flow algorithm (D8).

2) Throughout, I believe the authors are referring to "concentrated" subsurface lateral flow and should perhaps note that this is what they mean by "subsurface lateral flow."

We agree with this. So we added the word "concentrated" both in the title and the text.

3) It was not clear until late in the paper that the depths to the different soil discontinuities were determined manually, i.e., not by the soil survey. This needs to be made clearer and it throws doubt on the claim of "cost-effectiveness" noted in the conclusions. Also, I was left wondering if the surface topography alone would have sufficiently captured the flow paths?

This is a good point. We have re-examined the claim of "cost-effectiveness" and have modified the statements to better reflect the "hidden" costs associated with obtaining the necessary data for the GIS simulation. This is now incorporated into our new Discussion session as well as the expanded Conclusion section. We also indicated this in the revised Abstract section.

We mentioned that the depths to the three interfaces were determined and interpolated through 145 monitoring sites and 70 soil cores collected in the section 2.2 of "subsurface flow simulation" (page 2899 line 6 to 16 in HESSD). In order to address this issue more clearly, we now have moved this paragraph upward to the near-beginning of section 2.2. We also moved the description of soil cores collection and analysis in the section 2.3 "Data collections for validating simulated flow paths" (page 2901 line 17 to 20 in HESSD) into section 2.2 to clarify how these depths to different soil discontinuities were determined.

At present, the most detailed soil survey in the U.S. is so-called second-order soil survey. In this soil survey, the minimal size of delineation is 0.6 ha and the largest scale is 1:12,000 (Soil Survey Division, 1993). It does not contain adequate information of the depths to different soil discontinuities for the subsurface flow paths simulation in a study area like ours that is 19.5 ha in size. Therefore, we relied on our own local soil survey of the 145 or 70 soil cores to determine the depths to different soil discontinuities.

Since large quantity of soil cores were collected and analyzed, we can not say it was truly cost-effective to obtain those data. However, what we believe to be cost-effective is the D8 algorithm that was used to simulate the flow paths. Quite a few other studies have used other means to interpret the subsurface flow paths, for example, by dye tracing (e.g., Noguchi et al., 1999) and isotope (e.g., Asano et al., 2002). Comparing to these approaches, the D8 modeling itself is simple and cost-effective. In addition, as we discussed in the revised manuscript, if better ways of determining the subsurface soil discontinuities become available (e.g., using EMI, ground penetrating radar, or other geophysical tools), then the simulation of subsurface lateral flow path (as suggested in this study) can be more cost-effective.

In our study area and at the farm scale, the simulated flow paths at the three interfaces turned out to be nearly identical (>98% matched) since the variation in the topography of the three interfaces was much smaller compared to that of the variation in the surface topography across the entire study area (i.e., < 8.7% of the surface elevation change). Therefore, we would yield nearly identical results if the surface DEM was used in the simulation in this study (and we did test this, which turned out to be true). However, many other studies found the topography of subsurface interfaces to be quite different from the surface DEMs, and thus the flow path simulations based on the interface DEMs did yield better results than that using the surface DEMs (e.g., Freer et al., 2002; Burns et al., 1998). Thus, it is safer to say simulation based on the interface DEM should be used for predicting potential subsurface concentrated flow paths -- unless it is known that the interface topography varies similarly with the surface topography.

4) p5 end: consider using "finer" instead of "higher" resolution because it almost seems like "higher" refers to the larger numbers in (). Also, "better" is qualitative and misleading; consider substituting with "finer."

We have changed this as suggested.

5) I was unfamiliar with the Mn methodology used here. Consider a very brief description and justify method in the introduction instead of the in the results section.

We have improved this description as suggested.

6) Throughout the document, "relative" should be "relatively" as in several places on page 11, e.g. "In relatively dry…", "During the relatively dry…", and "In relatively wet conditions" – note, pluralizing "condition" also reads more easily.

We have changed this as suggested.

7) Page 12, first para: Note that the macropores would only transport water across the Ap1-Ap2 boundary during wet periods.

We have changed this as suggested.

8) "Morphological features" does not really capture the Mn corroboration. Consider revising to something like "Soil Mn distribution"

We have changed this as suggested.

Reviewer 3

General Comments:
I found the first 2 reviewers' comments well thought out and constructive. I do not really have any further remarks to make apart from a few technical issues. I think the manuscript should be published with some minor changes, particularly to some of the figures. In terms of structural changes, Reviewer #2 has made some pertinent comments that the authors should act on.

Thanks for the encouraging comments. The comments provided by the reviewer #2 have been followed as indicated above.

Specific Comments:
1) Specific Remarks p2899 L25. I also picked up on the use of "better" to describe the 3m DEM used in this study, this is a subjective remark that should be replaced by "of finer resolution".

We have changed this as suggested.

2) Also Fig 2 is probably taken from the ESRI manual for ARCGIS so should not be shown, it is common knowledge as pointed out by Reviewer#2.

We have modified this as suggested. However, Figure 2 is not only an illustration of the D8 algorithm, but also shows how we determine whether a monitoring site is on or off the simulated flow path. Therefore, we deleted the Figure 2 as suggested, but put an illustration of how we determine whether a soil moisture monitoring site is on or off the simulated flow path into the original Figure 3 (now Fig. 2d).

Technical Remarks:
1) P 2899 L26, Thompson is misspelt in the citation of their 2006 paper.

We have corrected this.

2) Figs 6 & 7 "Asterix" not "asteroid" should be in the caption

Thanks for noticing this. We think the "Asterix" is a typo of the reviewer #3. There is no such word in English dictionary. Reviewer #3 may mean "Asterisks". We have changed the "asteroid" into "Asterisks" in the caption of Figs. 6 and 7.

References cited:

Auerswald, K., Simon, S., and Stanjek, H.: Influence of soil properties on electrical conductivity under humid water regimes, Soil. Sci., 166, 382–390, 2001.

Burns, D.A., Hooper, R.P., McDonnell, J.J., Freer, J.E., Kendall, C., and Beven, K.: Base cation concentrations in subsurface flow from a forested hillslope: The role of flushing frequency, Water Resour. Res., 34, 3535–3544, 1998.

Freer, J., McDonnell, J.J, Beven, K.J., Peters, N.E., Burns, D.A, Hooper, R.P., Aulenbach, B., and Kendall, C.: The role of bedrock topography on subsurface storm flow, Water Resour. Res., 38, 1269, doi:10.1029/2001WR000872, 2002.

Gish, T.J., Walthall, C.L., Daughtry, C.S.T., and Kung, K.-J.S.: Using soil moisture and spatial yield patterns to identify subsurface flow pathways, J. Environ. Qual., 34, 274–286, 2005.

Krovchenko.: Influence of spatial structure on accuracy of interpolation methods, Soil Sci. Soc. Am. J., 67, 1564–1571, 2003.

Kravchenko, A.N. and Robertson, G.P.: Can topographical and yield data substantially improve total soil carbon mapping by regression kriging? Agron. J., 99, 12–17, 2007.

Noguchi, S., Tsuboyama, Y., Sidle, R.C., and Hosoda, I.: Morphological characteristics of macropores and the distribution of preferential flow paths in a forested slope segment, Soil Sci. Soc. Am. J., 63, 1413–1423, 1999.

Soil Survey Division Staff.: Soil Survey Manual, U.S. Department of Agriculture Handbook No. 18, U.S. Government Printing Office, Washington, DC, USA, 1993.

Simulation and Validation of Concentrated Subsurface Lateral Flow Paths in an Agricultural Landscape

Q. Zhu[1] and H.S. Lin[1]

[1]{The Pennsylvania State University, Department of Crop and Soil Sciences, 116 Agricultural Sciences and Industry Building, University Park, PA 16802, USA}

Correspondence to: H.S. Lin (henrylin@psu.edu)

Abstract

The importance of soil water flow paths to the transport of nutrients and contaminants has long been recognized. However, effective means of detecting subsurface flow paths in a large landscape is still lacking. The flow direction and accumulation algorithm based on the deterministic 8 single-flow method (D8) in GIS hydrologic modeling is a cost-effective way to simulate potential concentrated flow paths over a large area once relevant data are collected. This study tested the D8 algorithm for simulating concentrated lateral flow paths at three interfaces in soil profiles in a 19.5-ha agricultural landscape in central Pennsylvania, USA. These interfaces were (1) the interface between surface plowed layers of Ap1 and Ap2 horizons, (2) the interface with subsoil water-restricting clay layer where clay content increased to over 40%, and (3) the soil–bedrock interface. The simulated flow paths were validated through soil hydrologic monitoring, geophysical surveys, and observable soil morphological features. The results confirmed that concentrated subsurface lateral flow occurred at the interfaces with the clay layer and the underlying bedrock. At these two interfaces, the soils on the simulated flow paths were closer to saturation and showed more temporally unstable moisture dynamics than those off the simulated flow paths. Apparent electrical conductivity in the soil on the simulated flow paths was elevated and temporally unstable as compared to those outside the simulated paths. The soil cores collected from the simulated flow paths showed significantly higher Mn content at these interfaces than those away from the simulated paths. These results suggest that (1) the algorithm is useful in simulating possible concentrated subsurface lateral flow paths if used with appropriate threshold value of contributing area and sufficiently detailed digital elevation model; (2)

Deleted: based on the deterministic 8 method single-flow

Deleted: cost

Deleted: this

Deleted: (

Deleted:) interface

Deleted: s

Deleted: ly with

repeated electromagnetic surveys can reflect the temporal change of soil water storage and thus is a useful indicator of possible subsurface water movement over the landscape; and (3) observable Mn distribution in soil profiles can be used as a simple indicator of water flow paths in soils and over the landscape, but it does require sufficient soil sampling (by excavation or augering) to possibly infer landscape-scale subsurface flow paths.

Deleted: an
Deleted: soil
Deleted: content
Deleted: .

1 Introduction

Contribution of concentrated subsurface lateral flow in soils to rapid transport of nutrients and chemicals has been well recognized (e.g., Tsukamoto and Ohta, 1988; Elliot et al., 1998). Therefore, generating three-dimensional (3-D) scheme of subsurface flow paths in a landscape can help nutrient management and pollution control. However, limited means are available for detecting (especially nondestructively) subsurface flow paths in a large landscape. In addition, most studies on concentrated subsurface lateral flow reported in the literature have been conducted in forested catchments (e.g., Kitahara et al., 1994; Sidle et al., 2001; Lin et al., 2006), with much fewer studies conducted in agricultural landscapes.

Soil–bedrock interface has been recognized in a number of recent studies as an important concentrated subsurface lateral flow path. For example, Freer et al. (1997) reported a positive correlation between total flow volume and the contributing area calculated from a digital elevation model (DEM) of the soil–bedrock interface (instead of the soil surface). Noguchi et al. (1999) demonstrated through dye tracing that bedrock topography was important in contributing to preferential flow in a forested hillslope. Buttle and McDonald (2002) found that water flow at bedrock surface occurred in a thin saturated layer. Haga et al. (2005) demonstrated that saturated subsurface flow above soil–bedrock interface was dominant subsurface runoff. Fiori et al. (2007) also reported that the principal mechanism for the stream flow generation was subsurface flow along the soil–bedrock interface.

Deleted: s
Deleted: were

Because of often significant changes in texture, structure, or bulk density across the boundary of two adjacent soil horizons in a soil profile, soil horizon interface can also alter water flow direction and pattern (e.g., Kung, 1990, 1993; Ju and Kung, 1993; Gish et al., 2005). Several studies have reported water accumulation and subsequent lateral preferential flow above a high clay content and low hydraulic conductivity B horizon (called argillic horizon) (e.g., Haria et al., 1994; Perillo et al., 1999; Heppell et al., 2000). Slowly-permeable fragipans in many soils have also been recognized to develop seasonal perched water table and thus trigger

Deleted: s
Deleted: s

lateral preferential flow (e.g., Palkovics and Peterson, 1977; McDaniel et al., 2008). Because of compaction caused by farming equipments, plowpan (Ap2 horizon) underneath plowed layer (Ap1 horizon) can also potentially generate lateral seepage especially in rice paddy soils (e.g., Chen et al., 2002; Sander and Gerke, 2007). Sidle et al. (2001) also observed lateral flow at organic horizon–mineral soil interface in forested hillslopes.

Although concentrated subsurface lateral flow at the interfaces between soil horizons and between soil and underlying bedrock are important to water flow and chemical transport across a landscape, methods for effectively determining where and when concentrated subsurface lateral flow occurs remain very limited. In recent years, the flow direction and accumulation simulations based on DEM have been implemented in Geographic Information System (GIS) hydrologic modeling tools (e.g., Maidment, 2002). These simulations are based on the deterministic 8 method (D8) single-flow algorithm (also called nondispersive algorithm) (O'Callaghan and Mark, 1984). Although the D8 method has been widely used in the simulation of surface flow paths (e.g., Marks et al., 1984; Jones, 2002; Schäuble et al., 2008), it has not been widely used to simulate subsurface flow paths. Gish et al. (2005) have used this modeling tool to identify concentrated subsurface lateral flow paths above the clay layer in an agricultural watershed, which were confirmed by ground penetration radar (GPR) investigations. Bakhsh and Kanwar (2008) reported that flow accumulation generated from the D8 method contributed significantly to discriminate subsurface drainage clusters.

However, the D8 method only allows one of eight flow directions, which constrains the representation of flow path variability (Fairfield and Leymarie, 1991). Flow path simulated using the D8 tends to be concentrated to distinct, often artificially straight lines, as reported by Seibert and McGlynn (2007). In addition, Kenny et al. (2008) pointed out that the D8 algorithm can not yield good simulation results in low relief areas or areas with poor DEMs. Efforts to alleviate these drawbacks have focused on introducing models with multiple-flow directions, also called dispersive algorithms. For example, the algorithm proposed by Quinn et al. (1991) (MD8) distributes flow to all neighboring downslope cells weighted according to slope. However, dispersive algorithms produce numerical dispersion from a DEM cell to all neighboring cells with a lower elevation, which may be inconsistent with the physical definition of upstream drainage area (Orlandini et al., 2003). Tarboton (1997) proposed a nondispersive algorithm (Dinf) that assigns flow direction angle between 0 and 2π radian and allows an infinite number of possible flow directions. However, a certain degree of dispersion

Deleted: (

Deleted: ,

still remains in this method (Orlandini et al., 2003). According to Paik (2008), dispersive algorithms cannot define specific flow paths; therefore they are not suitable for investigating the transport of nutrient, pollutant, and water through channel corridors. In this respect, nondispersive algorithms (e.g., D8) are preferable. A few studies have suggested that the D8 method can yield good results in areas of substantial relief using a high resolution DEM (e.g., 3–5 m resolution DEM) (Guo et al., 2004; Kenny et al., 2008; Paik, 2008; Wu et al., 2008).

Soil apparent electrical conductivity (ECa) readings from electromagnetic induction (EMI) surveys are affected by soil properties such as clay content, soil water status, organic matter content, salinity, and depth to bedrock (Rhoades et al., 1976; Auerswald et al., 2001; Corwin and Lesch, 2005). Previous studies have used soil ECa from EMI surveys to represent soil water content. For example, Sherlock and McDonnell (2003) reported that soil ECa from EM38 (Geonics, Mississauga, Canada) vertical dipole mode could explain over 70% of gravimetrically determined soil-water variance. Reedy and Scanlon (2003) used the same sensor to explain 80% of the averaged volumetric water content in the soil profile. Although soil ECa values are affected by many soil properties, most of them (e.g., clay content, depth to bedrock, and organic matter content) are temporally stable over a relatively short period of time. Therefore, the temporal variation of soil ECa measured repeatedly within a short period of time (e.g., within a few months) should reflect the temporal variation in soil water content, after temperature correction (Zhu et al., 2009).

Soil morphological features (e.g., redox features, soil structure, macropores, and many others) are indicative of soil water movement (Lin et al., 2005). For example, previous studies have suggested that soil manganese (Mn) content is a good indicator of water movement in soil profiles. This is because Mn can be easily reduced and mobilized with moving water, and then oxidized and re-deposited when soil dries and O_2 reenters the soil (Patrick and Henderson, 1981). Yaalon et al. (1977) found that soil Mn content was topography and drainage related in three catenas. McDaniel and Buol (1991) and Walker and Lin (2008) reported greater soil Mn content at footslope and concave landscape positions because of water accumulation. Cassel et al. (2002) reported relationship between subsurface flow paths and dissolved Mn from higher to lower elevations on hillslopes. However, such simply indicator has not been utilized in larger scale studies (e.g., catchment and farm scales) to interpret subsurface water movement.

Deleted: paths,

Deleted: The s

Deleted: in the

Deleted: content

Deleted: the

Formatted: English (U.S.)

Deleted: quite a few

Formatted: English (U.S.)

Formatted: English (U.S.)

Deleted: comparatively

Deleted: several

Formatted: English (U.S.)

Deleted: of

Formatted: English (U.S.)

Formatted: English (U.S.)

Deleted: root

Deleted: were viewed as the signatures

Deleted: Mn

Deleted: was rarely

Deleted: used

Deleted: at the

Deleted: s

Deleted: the

Deleted: soil

The objective of this study was to investigate the reliability of high-resolution DEM-derived flow direction and accumulation algorithm (D8) implemented in ArcGIS 9.2 (ESRI, Redlands, CA, USA) for simulating concentrated subsurface lateral flow paths at three interfaces in a large agricultural landscape. The interfaces investigated included (1) the interface between the surface plowed layers of Ap1 and Ap2 horizons, (2) the interface between the upper soil profile and subsoil clay layer where clay content increased to over 40%, and (3) the interface between soil and the underlying bedrock. Three field indicators were then used to validate the simulated flow paths, including regular field soil moisture monitoring, EMI surveys, and soil Mn contents observed at these interfaces.

Deleted: an

Deleted: with

Deleted: electromagnetic induction (

Deleted:)

Deleted: manganese

2 Materials and Methods

2.1 Study site

This study was conducted in an agricultural landscape typical of the valley in the Northern Appalachian Ridges and Valleys physiographic region in the USA (Fig. 1). The 19.5-ha study area is located on The Pennsylvania State University's Kepler Farm in Rock Springs, PA. Typical crops grown on this farm are corn, soybean, and winter wheat. Elevation ranges from 373 m at the footslope in the northeastern corner to 396 m at the ridge top located in the middle portion of the field (Fig. 1). Depth to bedrock ranges from less than 0.25 m on the summit to more than 3 m on the footslope based on our field investigations. According to the second-order soil survey (Soil Survey Division Staff, 1993), five soil series have been identified in this landscape: the Hagerstown, Opequon, Murrill, Nolin, and Melvin soil series (Fig. 1). There are some transition zones among these soil series that we have identified on a refined soil map, including the Opequon-Hagerstown variant, Hagertown-Murrill variant, Hagerstown-Nolin variant, and Nolin-Melvin variant (Fig. 1). The dominant soil series are the Hagerstown silt loam (fine, mixed, semiactive, mesic Typic Hapludalfs) and the Opequon silty clay loam (clayey, mixed, active, mesic Lithic Hapludalfs). These are well-drained soils derived from limestone residuum, with the Hagerstown solum over 1.0 m thick and the Opequon solum < 0.5 m thick. The Murrill series (fine-loamy, mixed, semiactive, mesic Typic Hapludults) consists of deep, well-drained soils formed in sandstone colluvium with underlying residuum weathered from limestone. The Melvin silt loam (fine-silty, mixed, active, nonacid, mesic Fluvaquentic Endoaquepts) and the Nolin silt loam (fine-silty, mixed,

Deleted: , which has a delineated area of 19.5 ha

Deleted: of the hill

Deleted: second

Deleted: the

active, mesic Dystric Fluventic Eutrudepts) are deep soils formed in alluvium washed from surrounding uplands with limestone lying underneath the alluvium. The Nolin series is well-drained while the adjacent Melvin series is poorly drained (closer to a nearby stream).

2.2 Subsurface flow paths simulation

The DEMs of the three interfaces (the Ap1 to Ap2 interface, the interface with the clay layer, and the soil–bedrock interface) were generated by subtracting the land surface DEM (3-m resolution) by the Ap1 horizon thickness, depth to clay layer, and depth to bedrock, respectively. All spatial operations, including interpolations described below, were implemented using the ArcGIS.

A 1.1-m long intact soil core (0.038-m in diameter) was collected from each of 145 soil moisture monitoring sites when we installed PVC access tubes for soil moisture monitoring in this landscape (Table 1 and Fig. 1). The Ap1 horizon thickness was recorded from these 145 soil cores. Seventy out of these 145 soil cores were selected for determining clay content of each horizon and depth to clay layer where clay content increased to over 40% (Table 1 and Fig. 1). The clay content was analyzed using a simplified method proposed by Kettler et al. (2001). For the Nolin and Melvin series, the horizon with > 40% clay was not observed (27–29% clay in their B horizons); however, a restrictive horizon with greater density (>1.6 g/cm^3) was presented at the depth range of 0.6–1.0 m. For simplicity, we used the depth to this restrictive horizon in the Nolin and Melvin series (which only occupied a small portion of the overall landscape; see Fig. 1) to approximate their equivalent depth to clay layer. Ordinary kriging was used to generate the maps of the Ap1 horizon thickness and the depth to the clay layer. Both of these two soil properties had a small ratio of sample spacing over spatial correlation range (< 0.5) and a medium to strong spatial structure (nugget over sill ratio < 0.6). According to Kravchenko (2003) and Zhu and Lin (2009), these two soil properties can be reliably interpolated with ordinary kriging. Depth to bedrock was obtained from 77 point observations (Table 1 and Fig. 1), which showed a strong correlation with auxiliary variables such as terrain indices and ECa values obtained from EMI surveys (R^2 > 0.82). According to Kravchenko and Robertson (2007) and Zhu and Lin (2009), depth to bedrock can be better interpolated with regression kriging that incorporate the information of the auxiliary variables.

Potential concentrated lateral flow paths at the interfaces of Ap1–Ap2, clay layer, and soil–bedrock were simulated using the flow direction and accumulation algorithm implemented in

Deleted:

Deleted: the

Deleted: the

Deleted: the

Deleted: the

Deleted: map

Deleted: /

Deleted: y

Deleted: Regression kriging was used to interpolate the d

Deleted: .

Deleted: The depth to bedrock had

Deleted: (

Deleted: s)

Deleted: it

Deleted: se

Deleted: All spatial interpolations in this study were implemented using the ArcGIS Geostatistical Analyst.

Deleted: The DEMs of the three interfaces (the Ap1 to Ap2 interface, the interface with the clay layer, and the soil–bedrock interface) were generated by subtracting the land surface DEM (3-m resolution) by the Ap1 horizon thickness, depth to clay layer, and depth to bedrock, respectively. Depth to clay layer was defined as the depth to the first horizon with more than 40% clay. For the Nolin and Melvin series, the horizon with > 40% clay was not observed (27–29% clay in their B horizons); however, a restrictive horizon with greater density (>1.6 g/cm^3) was presented at the depth range of 0.6–1.0 m. For simplicity, we used the depth to this restrictive horizon in the Nolin and Melvin soils to approximate their depth to clay layer since these two soil series only occupied a small portion of the overall landscape.¶

Deleted: Ordinary kriging was used to generate the maps of the Ap1 horizon thickness from 145 soil cores collected from the study area, and the depth to clay layer map was generated from 70 of these soil cores (see Fig. 1 for the spatial locations of these soil cores). Regression kriging was used to interpolate the depth to bedrock from 77 point observations (Fig. 1). The selection of different spatial interpolation methods was based on a combined consideration of spatial structure and auxiliary variables (Zhu and Lin, 2009), i.e., soil properties with a small ratio of sample spacing over spatial correlation range (<0.5) should be interpolated with ordinary kriging, while soil properties with strong correlation with auxiliary variables (R^2>0.6) are better interpolated with regression kriging. All spatial interpolations in this study were implemented using the ArcGIS Geostatistical Analyst.¶

the ArcGIS 9.2 hydrologic modeling tool (Table. 2). This provides a grid of flow directions from one cell to its steepest downslope using the D8 single-flow algorithm. The flow accumulation determines the accumulated water from all cells in contributing area that flow into each downslope cell. Wu et al. (2008), via comparing different DEM resolutions (10, 30, 60, 90, 150, and 200 m), found that finer DEM resolution led to more accurate D8 simulation. The 3-m resolution DEM used in this study is finer than many previous studies reported in the literature (e.g., 5- and 10-m resolution DEMs in the studies of Erskine et al., 2006, and Thompson et al., 2006, respectively).

A threshold of contributing area was used to determine whether a cell was involved in a flow path. A smaller threshold indicates more cells participating in the flow. Thus, a smaller threshold is better for simulating flow paths under wet conditions, while a larger threshold is better suited for dry conditions. To date, no definitive model has emerged that provides clear criteria for selecting such threshold value. Besides, flow initiation mechanisms are likely to vary depending on local characteristics of climate, geology, soils, relief, and vegetation (e.g., Kirkby, 1994; Vogt et al., 2003). In the study of Gish et al. (2002), a threshold of 100 m^2 was suggested, while in the study of Bakhsh and Kanwar (2008), a threshold of 420 m^2 was used. In our study, instead of using a single threshold, we compared three thresholds of contributing area: 1,000, 500, and 100 m^2. The output from each flow simulation in the ArcGIS was a raster file, which was converted to a vector file for generating three buffer zones of 0–5, 5–10, and 10–15 m away from the simulated flow paths for comparing with the EMI survey data.

After flow path simulations, 145 monitoring sites were superimposed to determine whether a site was on or off the simulated flow paths (Fig. 2). If a monitoring site was in the cell of the simulated flow path or in the cell adjacent to the simulated path, it was considered as on the flow path; otherwise, it was considered as off the flow path (Fig. 2d). Since our DEM cell size was 3×3 m, if the maximal distance from a monitoring site to the simulated flow paths was less than 4.5 or 6.3 m (depending on orientation) (see Fig. 2d), then this site was considered to be on the flow path. Gish et al. (2005) used a similar criteria (< 5 m away from the simulated flow path) to determine whether a cell was on or off predicted lateral flow paths.

Deleted: The flow direction
Deleted: (see illustration in Fig. 2).
Deleted: higher
Deleted: better
Deleted: to
Deleted: simulate
Deleted: condition
Deleted: condition
Deleted: a
Deleted: in order to
Deleted: compare
Deleted: 3
Deleted: 2
Deleted: 2

2.3 Data collections for validating simulated flow paths

Three sets of data were collected in the field to validate the simulated flow paths. These were: (1) soil moisture monitoring (including volumetric soil water content and matric potential), (2) EMI surveys, and (3) observable soil Mn content at the three interfaces (Table 2).

Soil water content at multiple depths was monitored at 145 locations distributed throughout the study area (Fig. 1). These 145 sites covered all of the landforms and soil series in the study area (Table 1). Our procedure followed that used by Lin et al. (2006). Briefly, a portable TRIME-FM Time Domain Reflectomery (TDR) Tube Probe (IMKO, Ettlingen, Germany) was used to determine volumetric soil water content while being placed at specific depth interval in a PVC access tube installed at each site. Readings were taken at six depth intervals of 0–0.2, 0.1–0.3, 0.3–0.5, 0.5–0.7, 0.7–0.9, and 0.9–1.1 m (representing soil water content at 0.1, 0.2, 0.4, 0.6, 0.8, and 1.0 m depth, respectively). If the depth to bedrock at a monitoring site was not sufficiently deep to allow all six depth measurements, fewer readings were taken. For example, the actual numbers of subsoil water content observations were 110 and 96 for the 0.3–0.5 m and 0.7–0.9 m depth intervals, respectively. Entire study area's soil water content at these 145 sites was collected for 12 times from 2005 to 2007 (Table 3).

Seventy-four out of these 145 monitoring sites also had tensiometers installed (Fig. 1). These 74 locations were selected based on landforms and soil series in the study area (Table 1). Nested tensiometers were installed at five depths of 0.1, 0.2, 0.4, 0.8, and 1.0 m at each of these 74 sites. They were 0.15 m away from the TDR access tubes. Soil matric potentials along with soil water contents at these 74 locations were measured for 14 times from 2006 to 2008 (Table 3).

Seventy out of these 145 soil cores were selected for profile description (Fig. 1), including the quantity and size of visible pores, roots, and Mn mottles in each horizon (including that at the three interfaces). These morphological features were estimated visually following the standard soil survey procedures (Soil Survey Division Staff, 1993).

Soil ECa values were collected with EM38 sensor on four dates of 16 January, 10 March, 30 April, and 4 June of 2008. The EM38 sensor operated at a frequency of 13.2 KHz and provided effective theoretical measurement depths of 1.5 m when operated in vertical dipole mode. These EMI surveys were conducted with the same sample spacing of about 3×8 m (3-m spacing between two consecutive readings along each traverse line, and 8-m apart between traverse lines across the study area). We assumed that only soil moisture was changed during

Deleted: field data

Deleted: manganese (

Deleted:)

Deleted: farm

Deleted: These 145 sites covered all of the landforms and soil series in the study area (Table 1). At each site, r

Deleted: 1

Deleted: Whole farm

Deleted: s

Deleted: all

Deleted: were

Deleted: 2

Deleted: were also selected for

Deleted: installation

Deleted: 2

Deleted: A 1.1-m long intact soil core (0.038-m in diameter) was collected from each of the 145 soil moisture monitoring sites during the time when we installed the TDR access tubes.

Deleted: basic analysis and

Deleted: particle size distribution and

Deleted: Particle size distribution was analyzed using the method proposed by Kettler et al. (2001).

Deleted: procedure described in Soil

Deleted: Survey

Deleted: Manual for pores, roots, and redox, amount estimation

Deleted: Apparent electrical conductivity (

Deleted:)

Deleted: (Geonics, Mississauga, Canada)

Deleted: spatial resolution

Deleted: farm

Deleted: The readings in the EMI surveys are affected by soil properties such as clay content, moisture content, organic matter content, salinity, and depth to bedrock (Rhoades et al., 1976; Auerswald et al., 2001; Corwin and Lesch, 2005).

the period of our EMI surveys from January to June 2008 while other soil properties (e.g., clay content, depth to bedrock, and organic matter content) remained unchanged. Although temperature was also a changing factor, all EMI readings were corrected to a standard temperature of 25°C. Ordinary kriging was used to generate the ECa maps for the entire study area based on its spatial structure (Kravchenko, 2003; Zhu and Lin, 2009).

Deleted: pretty much

Deleted:

Deleted: EMI

2.4 Data analysis

For the 74 sites with both soil water content and matric potential measurements, soil water retention curves (SWRC) at different depths in each site were fitted with the model of van Genuchten (1980):

Deleted: monitoring

$$\frac{\theta(h)-\theta_r}{\theta_s-\theta_r}=\left[\frac{1}{1+(\alpha h)^n}\right]^{(n-1)/n}, \quad (1)$$

where α and n are empirical parameters; θ_s and θ_r are saturation and residual water contents, respectively; h is matric potential and $\theta(h)$ is volumetric water content under h. Examples of fitted SWRC for typical soil series, texture classes, and horizons in the study area are shown in Fig. 3. Texture class was one of the main factors affecting the shape of the SWRC. For example, in the Ap horizon, as the texture class changed from silty clay loam to silt loam, θ_s decreased from 0.43 to 0.37 m^3 m^{-3} (Fig. 3a, d, g). For the same texture class (e.g., silt loam) and soil series (e.g., the Murrill), θ_s decreased from 0.37 to 0.32 m^3 m^{-3} as the soil horizon changed from Ap to Bt2 (Fig. 3g, h, i). Because of plowing and root growth, surface soils had lower bulk density, more pore space, and thus greater θ_s than subsurface soils.

Deleted: 4

Deleted: 4a

Deleted: 4g

Volumetric soil water contents at the field capacity (0.33 kPa) and saturation (0 kPa) for each depth and each site were estimated through the fitted curve. The estimated water contents at field capacity ranged from 0.2 to 0.3 m^3 m^{-3}, while the estimated water contents at saturation ranged from 0.35 to 0.45 m^3 m^{-3} for the entire study area. The ratio of field capacity over saturation ranged from 0.60 to 0.65 (with a mean of 0.63). These estimated soil water contents at field capacity and saturation of all depths and all 74 sites were grouped according to their soil horizons (Ap, Bt1, and Bt2) and texture classes (silt loam, silty clay loam, and silty clay) (Fig. 4). The difference between Ap1 and Ap2 horizons was not considered here for two reasons: (1) the Ap1 horizon varied in thickness from 0.08 to 0.13-m in the study area; therefore, tensiometers installed at 0.1-m depth were located in the transition zones of Ap1 to Ap2 horizons; and (2) the TRIME-FM TDR probe was 0.18-m long, thus soil water

Deleted: the

Deleted: –

Deleted: 5

Deleted: in length

content of the Ap1 (0–0.1 m below the ground surface) and Ap2 (0.1–0.3 m) could not be clearly separated. Although the Ap2 horizon was denser than the Ap1 horizon, such density contrast was less strong as compared to that between Ap and Bt horizons in our study area.

For volumetric soil water content collected at each specific depth of each monitoring site, relative degree of saturation (*RS*) was calculated by dividing volumetric soil water content by the estimated saturated water content of this horizon and texture class (Fig. 4). A *RS* close to 1 suggests near saturation. At a specific soil horizon interface, 95% confidence intervals for the *RS* values between sites on and off the simulated flow paths were calculated using SAS (SAS Institute Inc., Cary, NC, USA). These confidence intervals were then compared using one-way ANOVA to determine whether significant differences in the *RS* existed between sites on and off the simulated flow paths (Table 2). Similarly, 95% confidence intervals of the *RS* values at, below, and above a specific interface (Ap1–Ap2, clay layer, or soil–bedrock) were also compared to determine whether significant statistical differences existed (Table 2).

At each interface, temporal stability of the *RS* values of all 145 monitoring sites was analyzed using the approach proposed by Vachaud et al. (1985):

$$R_j = \frac{1}{N}\sum_{i=1}^{N} R_{ij}, \quad (2)$$

$$\delta_i = \frac{1}{M}\sum_{j=1}^{M}\left(\frac{R_{ij} - R_j}{R_j}\right), \quad (3)$$

$$S_\delta = \sqrt{\frac{1}{M}\sum_{j=1}^{M}\left(\delta_{ij} - \delta_i\right)^2}, \quad (4)$$

where R_j is the arithmetic mean of *RS* at all sites in day *j*; R_{ij} is the *RS* of a particular interface at site *i* in day *j*; *N* is the number of monitoring sites (in this study, $N = 145$); δ_i is the arithmetic mean of the relative difference of *RS* at site *i*; *M* is the number of times that the whole study area's soil water content was measured (in this study, $M = 12$); and S_δ is the standard deviation of δ_i. Positive or negative δ_i suggests that at a particular interface, site *i* is wetter or dryer, respectively, than the average condition of the entire study area. The S_δ depicts the magnitude of temporal stability of *RS* at a particular interface at site *i*. Higher S_δ indicates a more dynamic change (i.e., temporally unstable) in soil moisture. Temporal stability of the *RS* values between sites on and off the simulated flow paths was also compared at each interface (Table 2)

Deleted: below the ground surface
Deleted: the
Deleted: it
Deleted: 5
Formatted: Font: Italic
Deleted: Table 3
Deleted: Table 3
Deleted: stabilities
Deleted: were
Deleted: farm
Deleted: farm
Deleted: , respectively
Deleted: stabilities
Deleted: were
Deleted: Table 3

Following the same procedure, we conducted the temporal stability analysis of ECa values collected in four EMI surveys. Temporal stability of ECa in the three buffer zones (0–5, 5–10, and 10–15 m away from the simulated flow paths) and the rest of the study area were statistically compared with each other through t-test in SAS (p<0.05) (Table 2). The temporal changes in ECa reflected the change in soil water content. Therefore, the magnitude of ECa temporal stability can represent the degree of change in soil water storage in the three buffer zones of the predicted flow paths vs. the rest of the study area.

At the three interfaces, Mn contents estimated from soil cores were also statistically compared between sites on and off the simulated paths through t-test in SAS (p<0.05) (Table 2). The Mn mass observed in the soil is an indicator of soil water movement as demonstrated in other studies (e.g., McDaniel et al., 2008; Walker and Lin, 2008).

3 Results

3.1 Simulated subsurface flow paths

The spatial patterns of potential lateral flow paths at the three interfaces simulated with different thresholds of contributing area (i.e., 100, 500, and 1,000 m^2) are illustrated in Fig. 2a–c for the soil–bedrock interface, where the patterns using the thresholds of 1,000 and 500 m^2 were close to each other but quite different from that using the threshold of 100 m^2. Because of the topography of the study area, very few locations (< 8% of the entire area) had a contribution area > 500 m^2. Therefore, the simulated flow paths using the threshold contribution areas of 1,000 and 500 m^2 were sparse and similar. In comparison, 25% cells of the entire study area had contribution area > 100 m^2. In the subsequent analysis, we focus on comparing the simulated flow paths obtained with 500 and 100 m^2 thresholds. In Fig. 2a–c, water moved laterally across the landscape through the soil–bedrock interface in three main areas: the north-east corner, the mid-west depressional area, and the mid-south portion. When using a smaller threshold (100 m^2), more areas participated in the flow, leading to 61% of the soil water monitoring sites (total 88 sites) being identified as on the simulated flow paths (Fig. 2c). In contrast, during drier conditions using a larger threshold of 500 m^2, only 35% of the 145 monitoring sites were identified as on the simulated flow paths (Fig. 2b).

In the study area, the maximum difference in surface elevation was 23 m between the lowest point in the footslope and the highest point at the ridge top. However, the largest differences

Deleted: stabilities

Deleted: Table 3

Deleted: studied

Deleted: Table 3

Deleted: This is because Mn can be easily reduced and mobilized with moving water, and then oxidized and re-deposited when soil dries and O_2 reenters the soil (Patrick and Henderson, 1981). Therefore, high Mn concentration often indicates water flow paths.

Deleted: and Discussions

Deleted: 3

Deleted: 3

Deleted: out of

Deleted: paths

Deleted: 3c

Deleted: condition

Deleted: 3b

Deleted: in

in the Ap1 horizon thickness and depths to the clay layer and the bedrock for the entire landscape were less than 2 m (i.e., < 8.7% of the surface elevation change). Consequently, the topography of the three interfaces was dominated by the variation in land surface elevation, resulting in similar spatial patterns in the simulated lateral flow paths among the three interfaces.

3.2 Validating the simulated flow paths through soil hydrologic monitoring

At each of the three interfaces, the *RS* values between the monitoring sites on and off the simulated flow paths were statistically compared (Table 2). In relatively dry conditions (average volumetric soil water content $\bar{\theta}$ at the interfaces with the clay layer or bedrock was smaller than 0.28 and 0.31 m^3 m^{-3}, respectively), the *RS* values of the sites on the simulated flow paths (500 m^2 threshold) were significantly greater (p<0.05) than those sites off the paths (Fig. 5b, c). However, this was not the case at the Ap1–Ap2 interface (Fig. 5a). In relatively wet conditions ($\bar{\theta}$>0.28 and 0.31 m^3 m^{-3} at the interfaces with the clay layer or bedrock, respectively), significant difference (p<0.05) in the *RS* values also existed between the sites on and off the simulated flow paths (100 m^2 threshold) at the interfaces with the clay layer or bedrock (Fig. 5b, c), but not at the Ap1–Ap2 interface (Fig. 5a).

To further verify the water accumulation at the clay layer interface, the *RS* values at this interface were statistically compared with the *RS* values right below this interface and 0.2-m above this interface (Fig. 6a). In relatively dry conditions ($\bar{\theta}$<0.28 m^3 m^{-3}), the *RS* values at this interface for the sites on the simulated flow paths (500 m^2 threshold) were significantly greater (p<0.05) than that above and below it. In relatively wet conditions ($\bar{\theta}$>0.28 m^3 m^{-3}), such significant difference (p<0.05) in the *RS* values also existed between the sites on and off the flow paths simulated with the threshold of 100 m^2. For the sites off the simulated flow paths, differences in the *RS* values between the clay layer interface and that above or below the interface were not significant under either dry or wet conditions (Fig. 6a).

For sites on the flow paths simulated with the threshold of 100 m^2, the *RS* values at the soil–bedrock interface were significantly greater (p<0.05) than those 0.2-m above it, regardless of the wetness condition (Fig. 6b). In comparison, for sites on the flow paths simulated with the threshold 500 m^2, significant difference in the *RS* values between the soil–bedrock interface and 0.2-m above it could only be observed in relatively dry conditions ($\bar{\theta}$<0.31 m^3 m^{-3}).

Deleted: of
Deleted: in
Deleted: nearly identical
Deleted: In the study of Birkhead et al. (1996), the bedrock topography derived from GPR image was also shown to be closely related to the surface topography (elevations of bedrock and ground surface decreased simultaneously for about 1.5 m in a 90-m transect).
Deleted: relative
Deleted: condition
Deleted: and soil–
Deleted: interfaces
Deleted: ere
Deleted: at both clay layer and soil–bedrock interfaces
Deleted: 6b
Deleted:),
Deleted: but not at
Deleted: 6a
Deleted: During the relative dry period, more drainage areas were required to initiate the lateral subsurface flow upon rainfall inputs. Thus, a greater threshold (e.g., 500 m^2) simulated better the potential lateral flow paths. ¶
Deleted: relative
Deleted: condition
Deleted: clay layer and soil–bedrock interfaces
Deleted: both
Deleted: and soil–
Deleted: interfaces
Deleted: 6b
Deleted: , again,
Deleted: 6a
Deleted: In our study area, the s ... [1]
Deleted: Unlike the *RS* values a ... [2]
Deleted: 7a
Deleted: relative
Deleted: condition
Deleted: relative
Deleted: condition
Deleted: it
Deleted: in
Deleted: 7a
Deleted: 7b
Deleted: condition
Deleted: This further suggests th ... [3]

The temporal stability of the *RS* values between the sites on and off the simulated flow paths (100 m^2) at all three interfaces were compared in Fig. 7. At the clay layer and soil–bedrock interfaces, sites on the simulated flow paths had greater relative differences of *RS* and standard deviations than the sites off the flow paths (Fig. 7b, c), suggesting a more dynamic (and thus unstable) moisture status over time for the sites on the flow paths. At the clay layer interface, 70% of the sites on the flow paths had δ_i >0 and 75% of them had standard deviation of δ_i >0.1, while only 13% and 36% of the sites off the flow paths had δ_i >0 and standard deviation of δ_i >0.1, respectively. At the soil–bedrock interface, percentages of the sites on the flow paths with positive δ_i value and high standard deviation (>0.1) were even greater, 85% and 90%, respectively, while the corresponding percentages were only 12% and 36% for the sites off the flow paths. At the Ap1–Ap2 interface, the sites on and off the simulated flow paths had no distinct differences in δ_i (Fig. 7a). When flow path threshold was changed to 500 m^2, results similar to that shown in Fig. 7 were observed (data not shown).

3.3 Validating the simulated flow paths through repeated EMI surveys

The temporal stability of ECa values in different buffer zones of the simulated flow paths is shown in Fig. 8, with a threshold of 500 m^2. As the distance from the simulated flow paths increased, both the mean and standard deviation of the relative difference in ECa decreased, suggesting that the soils closer to the simulated flow paths tended to have elevated and more dynamic ECa values. Additionally, the positive relative differences in ECa in the three buffer zones (0–5, 5–10, and 10–15 m) imply that their ECa values were greater than the overall average of the entire landscape. The greater standard deviations further suggest that the soil ECa values in areas closer to the simulated flow paths had higher temporal variations than the soils further away from these flow paths (Fig. 8).

3.4 Validating the simulated flow paths through soil Mn distribution

The simulated flow paths were further validated through the spatial variation in soil Mn contents at the clay layer and soil–bedrock interfaces (Table 2 and Fig. 9). For the sites on the simulated flow paths (threshold of 500 m^2), soils Mn content at these two interfaces were generally greater than 1% and reached as high as 5–10% at some locations. However, for the sites off the simulated flow paths, almost no Mn was observed at these two interfaces. Therefore, locations with greater soil Mn content are expected to be on or closer to subsurface flow paths.

Deleted: 9

Deleted: 9b

Deleted: layer

Deleted: This observation indicates that the clay layer and soil-bedrock interfaces at the sites on the simulated flow paths were largely wetter and more temporally unstable, implying more water movement through these interfaces in general. De Lannoy et al. (2006) also documented that subsurface lateral flow resulted in high temporal variability of soil water content at the clay layer interface.

Deleted: 9a

Deleted: When

Deleted: s

Deleted: (100 m^2) in Fig.

Deleted: 9

Deleted: 7 was

Deleted: similar

Deleted: 10

Deleted: ir

Deleted: 10

Deleted: Previous studies have used soil ECa values to represent soil water content. Sherlock and McDonnell (2003) reported that soil ECa measurements using EM38 vertical dipole mode could explain over 70% of gravimetrically determined soil-water variance. Reedy and Scanlon (2003) also used the same sensor to explain 80% of the averaged volumetric water content in the soil profile. We assumed that the change in soil water content was the main control of the temporal variation in ECa values during our repeated EMI surveys from January to June 2008 (note that all temperatures were corrected to a standard value). Therefore, the higher and more unstable soil ECa values in areas closer to the simulated flow paths suggest increased wetness and more dynamic moisture changes.¶

Formatted: Bullets and Numbering

Deleted: morphological features

Deleted: 11

Deleted: Other studies have suggested that soil Mn content is a good indicator of water movement in soil profiles. For example, Yaalon et al. (1977) found that soil Mn content was topography and drainage related in three catenas. McDaniel and Buol (1991) and Walker and Lin (2008) reported greater soil Mn content at footslope and concave landscape positions because of water accumulation. Cassel et al. (2002) reported relationship between subsurface flow paths and dissolved Mn from higher to lower elevations on hillslopes.

4 Discussion

The flow paths simulated with the DEMs of the three interfaces and the DEM of the land surface were nearly identical in this study, with over 98% of the simulated flow paths being the same. This suggested that the flow path simulations were not improved with the consideration of the subsurface interfaces' DEMs in this particular landscape. Similar results were reported by Birkhead et al. (1996), in which the bedrock topography derived from GPR image was shown to be closely related to the surface topography (elevations of bedrock and ground surface decreased simultaneously for about 1.5 m in a 90-m transect). However, other studies observed that the topography of subsurface interfaces could be quite different from that of the land surface and thus the simulation based on the interfaces' topography yielded better results. For example, Freer et al. (2002) found that terrain attributes of the land surface did not capture the observed spatial patterns of hillslope hydrologic response, while the bedrock surface topography significantly improved the interpretation of flow spatial variation. Burns et al. (1998) documented that accumulated area simulated with the bedrock surface DEM explained better the base cation concentrations in the subsurface flow. Therefore, subsurface simulation based on the DEMs of subsurface interfaces is more reliable – unless it is known that the subsurface interface topography varies similarly with the surface topography. Thus, it is desirable to find ways to predict the depth to subsurface water-restricting layers (such as the clay layer or the bedrock) so that the cost-effectiveness of the GIS modeling could be better realized.

Our hydrological monitoring suggested that concentrated lateral flow paths at the interfaces with the clay layer or the bedrock were reasonably simulated with the D8 algorithm. First, soils on the simulated flow paths at these two interfaces were closer to saturation than those off the paths (Fig. 5b, c). Second, for sites on the simulated flow paths, soils at these two interfaces were also closer to saturation than soils below or above these interfaces (Fig. 6). Third, the temporal stability analysis indicated that the interfaces with the clay layer or the bedrock on the simulated flow paths were largely wetter and more temporally unstable (Fig. 7b, c), implying generally more water movement through these interfaces. De Lannoy et al. (2006) also documented that concentrated subsurface lateral flow resulted in high temporal variability of soil water content at the clay layer interface.

Deleted: s
Deleted: se
Deleted: nearly identical
Deleted: .
Deleted: More than
Deleted: se
Deleted: at the three interfaces and land surface were the exactly
Deleted: case
Deleted: .
Deleted: Similar
Deleted:
Deleted: as
Deleted:
Deleted: in the study of
Deleted: a few
Deleted: was strongly
Deleted: the topography of
Deleted: se
Deleted: ed
Deleted: (upslope length)
Deleted: trench flow
Deleted: estimation
Deleted: of flow
Deleted: better
Deleted: the
Deleted: interface
Deleted: necessary
Deleted: since it yields the result no worse than using the surface DEM
Deleted: and in many cases, it is hard to determine whether the interface topography was sufficiently different from the surface topography
Deleted: and soil–
Deleted: interfaces
Deleted: successfully
Deleted: at these two interfaces,
Deleted: on the
Deleted: two
Deleted: and
Deleted: soil–
Deleted: interfaces at the sites
Deleted: in general

Our hydrological monitoring also indicated that lateral subsurface flow did not exist at the Ap1–Ap2 interface. No significant difference in the *RS* values was observed between the sites on and off the simulated flow paths at the Ap1–Ap2 interface (Fig. 5a). In addition, the temporal stability between sites on and off the simulated flow paths had no distinct differences at this interface (Fig. 7a). The interfaces of different soil horizons can trigger lateral subsurface flow as reported in some previous studies (e.g., Kung, 1990, 1993; Ju and Kung, 1993; Gish et al., 2005). However, as shown in this study, not all interfaces are effective in generating lateral subsurface water flow in agricultural landscapes. When describing soil cores in this study, we noticed that the surface horizons (e.g., Ap1 and Ap2) were biologically active and had many macrospores (earthworm holes and root channels). These macrospores could have transported water from the Ap1 to Ap2 horizon without much restriction during wet periods and thus prevented the water from accumulating at this Ap1-Ap2 interface. Another possible reason for the lack of lateral flow between the Ap1 to Ap2 horizons was the possible limitation of the monitoring devices used to determine soil moisture in these two horizons (i.e., the 0.18-m long TDR probe overlapped the Ap1 and Ap2 horizons' readings and some tensiometers were located in the transition zones between the Ap1 to Ap2 horizons). In comparison, clay-enriched argillic horizon or dense fragipan have been widely recognized as important lateral flow paths in subsoils (e.g., Heppell et al., 2000; Gish et al., 2005; Lin et al., 2008). The clay layer interface was generally deeper than 0.4 m in our study area. At such depth, fewer macrospores were observed and thus the vertical water percolation could be more restricted.

The repeated EMI surveys suggested that the spatial pattern of subsurface lateral flow paths simulated with GIS was reasonable and compared favorably with the ECa data. We assumed that the change in soil water content was the main control of the temporal variation in ECa values during our repeated EMI surveys from January to June 2008 (note that all temperatures were corrected to a standard value). This is consistent with some previous studies that reported strong correlation between soil ECa and soil water storage (e.g., Sherlock and McDonnell, 2003; Reedy and Scalon, 2003). Thus, the higher and more unstable ECa values in areas closer to the simulated flow paths (Fig. 8) suggest that the wetness there was increased and moisture dynamics was more significant. However, because we used approximately 8-m line spacing in our EMI surveys, specific subsurface lateral flow paths could not be clearly identified on our EMI maps. To do so would require denser line spacing

Deleted: ies

Deleted: by

Deleted: were

Deleted: active

Deleted: transport

Deleted: the

Deleted: near

Deleted: plenty of

Deleted: were observed in them

Deleted: in

Deleted: the

Deleted: contrast

Deleted: the

Deleted: and

Deleted: the

Deleted: were both

Deleted: identified to be

Deleted: in this study and previous studies

Deleted: (fragipan)

Deleted: the

Deleted: lateral

Deleted: was captured through our simulation

Deleted: was according to

Deleted: the

Deleted: erefore

Deleted: increased

Deleted: more dynamic

Deleted: changes

(e.g., ≤1 m) and perhaps also shorter time intervals (e.g., right before and after a large rainstorm) for repeating EMI surveys.

Soil morphological features (Mn distribution in soils) further justified the existence of subsurface lateral flow at the interfaces with the clay layer and the bedrock as such flow paths simulated with GIS matched with the observed Mn content distribution in the soils in the study area. Previous studies have suggested that soil Mn content is a good indicator of water movement in soil profiles (e.g., Yaalon et al., 1977; McDaniel and Buol, 1991; Cassel et al., 2002; Walker and Lin, 2008). In our study, high Mn content was observed at the interfaces with the clay layer and the bedrock on the simulated flow paths, whereas soil Mn content off the simulated flow paths was almost zero (Fig. 9).

During the relatively dry period, more drainage areas were required to initiate the lateral subsurface flow upon rainfall inputs. Thus, a larger threshold (e.g., 500 m^2) simulated better the potential lateral flow paths at the clay layer interface (Fig. 5b). In contrast, during the wet period, a smaller threshold (e.g., 100 m^2) was better to simulate the potential lateral flow paths at this interface (Fig. 5b). In our study area, the soil water content generally increased with depth and often reached the highest value at the soil–bedrock interface. Even during relatively dry period, the soil at the soil–bedrock interface might still be wet and free water lateral movement could occur after large rainstorms. In such case, a smaller threshold of 100 m^2 could still reasonably simulate concentrated lateral subsurface flow paths at the soil–bedrock interface. This is supported by significant differences in the *RS* between the sites on and off the simulated flow paths (threshold 100 m^2) during the dry period, as shown in Fig. 5c. In addition, significant differences between soil water content at the soil–bedrock interface and 0.2 m above it can also be observed for sites on the simulated flow paths (threshold 100 m^2) during the dry period (Fig 6b). This further suggests that a smaller threshold (100 m^2) works better to simulate flow paths at the soil–bedrock interface under both dry and wet conditions.

Deleted: content

Deleted: lateral

Deleted: soil–

Deleted: interfaces and

Deleted: were successfully

Deleted: this study

Deleted: ; Cassel et al., 2002

Deleted: also

Deleted: se two

Deleted: (Fig. 9)

Deleted: In addition to Mn content, some other soil morphological features including redox mottle, soil structure, pores and roots can also be used as indicators of soil water movements (Lin et al., 2005)

Deleted: also

Deleted: some

Deleted: in

5 Conclusions

Through validation by soil hydrologic monitoring, EMI surveys, and soil morphological observations, it was apparent that concentrated subsurface lateral flow occurred at the interfaces with the clay layer (or water-restrictive layer) and the underlying bedrock in the

agricultural landscape studied, but not at the interface between the surface plowed layers of Ap1 and Ap2 horizons (because of considerable biological activities at that interface and the likely limitation of the monitoring devices used that could not clearly separate the two horizons' soil moisture dynamics). The ArcGIS hydrologic modeling (the D8 algorithm) did a reasonable job in simulating potential concentrated lateral flow paths at the interfaces in soil profiles. Such simulated subsurface lateral flow paths were temporally dynamic as they varied with the wetness condition of the landscape. Hence, using different thresholds of contributing area for the GIS hydrologic simulation would be needed to obtain expected results under different moisture conditions (e.g., 500 m^2 for relatively dry conditions and 100 m^2 for relatively wet conditions in this study). Sufficiently detailed DEM is also needed to ensure that the GIS flow algorithm performs with lower uncertainty. We suggest additional testing of this cost-effective means of predicting likely subsurface flow paths in other landscapes in order to establish a solid protocol for simulating subsurface hydrologic flow paths in different watersheds. However, some costs would incur in obtaining necessary data for such simulation to be effective. Thus, finding means of predicting the depth to subsurface water-restricting layers (such as the clay layer or the bedrock) will enhance the cost-effectiveness of the GIS modeling approach. In areas where subsurface interface topography vary similarly with the surface topography, the surface DEM could be used to approximate the subsurface interface topography to obtain similar results. Repeated EMI surveys provide another low-cost and nondestructive means of detecting potential concentrated subsurface flow paths; however, dense sample spacing and frequently repeated surveys would be needed if specific subsurface flow paths are to be identified via repeated EMI surveys. While soil morphological features such as Mn distribution in soil profiles also serve as useful indicators of subsurface water flow paths, it does require soil sampling (by excavation or augering) with sufficient numbers of observations to possibly infer landscape-scale subsurface flow paths.

Deleted: the

Deleted: se

Deleted:

Deleted: , however,

Deleted: condition

Deleted: condition

Deleted: could also

Acknowledgements

This research was partially supported by the USDA Higher Education Challenge Competitive Grants Program (Grant no. 2006-38411-17202).

References

Auerswald, K., Simon, S., and Stanjek, H.: Influence of soil properties on electrical conductivity under humid water regimes, Soil. Sci., 166, 382–390, 2001.

Bakhsh, A. and Kanwar, R.S.: Soil and landscape attributes interpret subsurface drainage clusters, Aust. J. Soil. Res., 46, 735–744, 2008.

Birkhead, A.L., Heritage, G.L., White, H., and van Niekerk, A.W.: Ground-penetrating radar as a tool for mapping the phreatic surface, bedrock profile, and alluvial stratigraphy in the Sabie River, Kruger National Park, J. Soil Water Cons., 51, 234–241, 1996.

Burns, D.A., Hooper, R.P., McDonnell, J.J., Freer, J.E., Kendall, C., and Beven, K.: Base cation concentrations in subsurface flow from a forested hillslope: The role of flushing frequency, Water Resour. Res., 34, 3535–3544, 1998.

Buttle, J.M. and McDonald, D.J.: Coupled vertical and lateral preferential flow on a forested slope, Water Resour. Res., 38, 1060, doi:10.1029/2001WR000773, 2002.

Cassel, D.K., Afyuni, M.M., and Robarge, W.P.: Manganese distribution and patterns of soil wetting and depletion in a piedmont hillslope, Soil Sci. Soc. Am. J., 66, 939–947, 2002.

Chen, S.K., Liu, C.W., and Huang, H.C.: Analysis of water movement in paddy rice fields (II) simulation studies, J. Hydrol., 268, 259–271, 2002.

Corwin, D.L. and Lesch, S.M.: Apparent soil electrical conductivity measurements in agriculture, Comput. Electron. Agr., 46, 11–43, 2005.

De Lannoy, G.J.M., Verhoest, N.E.C., Houser, P.R., Gish, T.J., and van Meirvenne, M.: Spatial and temporal characteristics of soil moisture in an intensively monitored agricultural field (OPE3), J. Hydrol., 331, 719–730, 2006.

Elliot, J.A., Cessna, A.J., Best, K.B., Nicholaichuk, W., and Tollefson, L.C.: Leaching and preferential flow of clopyralid under irrigation: field observations and simulation modeling, J. Environ. Qual., 27, 124–131, 1998.

Erskine, R.H., Green, T.R., Ramirez, J.A., and MacDonald, L.H.: Comparison of gridbased algorithms for computing upslope contributing area, Water Resour. Res., 42, W09416, doi:10.1029/2005WR004648, 2006.

Fairfield, J. and Leymarie, P.: Drainage networks from grid digital elevation models, Water Resour. Res., 27, 709–717, 1991.

Fiori, A., Romanelli, M., Cavalli, D.J., and Russo, D.: Numerical experiments of streamflow generation in steep catchments, J. Hydrol., 339, 183–192, 2007.

Freer, J., McDonnell, J.J, Beven, K.J., Brammer, D., Burns, D.A, Hooper, R.P., and Kendall, C.: Topographic controls on subsurface storm flow at the hillslope-scale for two hydrologically distinct small catchments, Hydrol. Processes., 11, 1347–1352, 1997.

Freer, J., McDonnell, J.J, Beven, K.J., Peters, N.E., Burns, D.A, Hooper, R.P., Aulenbach, B., and Kendall, C.: The role of bedrock topography on subsurface storm flow, Water Resour. Res., 38, 1269, doi:10.1029/2001WR000872, 2002.

Gish, T.J., Dulaney, W.P., Kung, K.-J.S., Daughtry, C.S.T., Doolittle, J.A., and Miller, P.T.: Evaluating use of ground-penetrating radar for identifying subsurface flow pathways, Soil Sci. Soc. Am. J., 66, 1620–1629, 2002.

Gish, T.J., Walthall, C.L., Daughtry, C.S.T., and Kung, K.-J.S.: Using soil moisture and spatial yield patterns to identify subsurface flow pathways, J. Environ. Qual., 34, 274–286, 2005.

Guo, J. H., Liang, X., and Leung, L.R.: A new multiscale flow network generation scheme for land surface models, Geophys. Res. Lett., 32, L23502, doi:10.1029/2004GL021381, 2004.

Haga, H., Matsumoto, Y., Matsutani, J., Fujita, M., Nishida, K., and Sakamoto, Y.: Flow paths, rainfall properties, and antecedent soil moisture controlling lags to peak discharge in a granitic unchanneled catchment, Water Resour. Res., 41, W12410, doi:10.1029/2005WR004236, 2005.

Haria, A.H., Johnson, A.C., Bell, J.P., and Batchelor, C.H.: Water-movement and isoproturon behaviour in a drained heavy clay soil. 1. Preferential flow processes, J. Hydrol., 163, 201–216, 1994.

Heppell, C.M., Burt, T.P., and Williams, R.J.: Variations in the hydrology of an underdrained clay hillslope, J. Hydrol., 227, 236–256, 2000.

Jones, R.: Algorithms for using a DEM for mapping catchment areas of stream sediment samples, Comput. Geosci., 28, 1051–1060, 2002.

Ju, S.H. and Kung, K.-J.S.: Finite element simulation of funnel flow and overall flow property induced by multiple soil layers, J. Environ. Qual., 22, 432–442, 1993.

Kenny, F., Matthews, B., and Todd, K.: Routing overland flow through sinks and flats in the interpolated raster terrain surfaces, Comput. Geosci., 34, 1417–1430, 2008.

Kettler, T.A., Doran, J.W., and Gilbert, T.L.: Simplified method for soil particle-size determination to accompany soil-quality analyses, Soil Sci. Soc. Am. J., 65, 849–852, 2001.

Kirkby, M.J.: Thresholds and instability in stream head hollows: a model of magnitude and frequency for wash processes, in: Process Models and Theoretical Geomorphology, edited by: Kirkby, M.J., Wiley, Chichester, 295–314, 1994.

Kitahara, H, Terajima, T., and Nakai, Y.: Ratio of pipe flow to throughflow discharge, J. Jpn. Forest. Soc., 76, 10–17, 1994.

Krovchenko.: Influence of spatial structure on accuracy of interpolation methods, Soil Sci. Soc. Am. J., 67, 1564–1571, 2003.

Kravchenko, A.N. and Robertson, G.P.: Can topographical and yield data substantially improve total soil carbon mapping by regression kriging? Agron. J., 99, 12–17, 2007.

Kung, K.-J.S.: Preferential flow in a sandy vadose zone: 1. Field observation, Geoderma, 46,

30 51–71, 1990.

Kung, K.-J.S.: Laboratory observation of the funnel flow mechanism and its influence on solute transport, J. Environ. Qual., 22, 91–102, 1993.

Lin, H.S., Bouma, J., Wilding, L.P., Richardson, J.L., Kutilek, M., and Nielsen, D.R.: Advances in hydropedology, Adv. Agron., 85, 1–89, 2005.

Deleted: .

Lin, H.S., Kogelmann, W., Walker, C., and Bruns, M.A.: Soil moisture patterns in a forested catchment: A hydropedological perspective, Geoderma, 131, 345-368, 2006.

Lin, H.S., Brook, E., McDaniel, P., and Boll, J.:Hydropedology and Surface/Subsurface Runoff Processes. In M. G. Anderson (Editor-in-Chief) Encyclopedia of Hydrologic Sciences. John Wiley & Sons, Ltd. DOI: 10.1002/0470848944.hsa306, 2008.

Maidment, D.: Arc Hydro: GIS for Water Resources, ESRI, Redlands, CA, USA, 2002.

Marks, D., Dozier, J., and Frew, J.: Automated basin delineation from digital elevation data, GeoProcessing, *2*, 299–311, 1984.

McDaniel, P.A. and Buol, S.W.: Manganese distributions in acid soils of the North Carolina Piedmont, Soil Sci. Soc. Am. J., 55,152–158, 1991.

McDaniel, P.A., Regan, M,P., Brooks, E., Boll, J., Bamdt, S., Falen, A., Young, S.K., and Hammel, J.E.: Linking fragipans, perched water tables, and catchment-scale hydrological processes, Catena, 73, 166–173, 2008.

Noguchi, S., Tsuboyama, Y., Sidle, R.C., and Hosoda, I.: Morphological characteristics of macropores and the distribution of preferential flow paths in a forested slope segment, Soil Sci. Soc. Am. J., 63, 1413–1423, 1999.

O'Callaghan, J.F. and Mark, D.M.: The extraction of drainage networks from digital elevation data, CVGIP, 28, 323–344. 1984.

Orlandini, S., Moretti, G., Franchini, M., Aldighieri, B., and Testa, B.: Path-based methods for the determination of nondispersive drainage directions in grid-based digital elevation models, Water Resour. Res., 39, 1144, doi:10.1029/2002WR001639, 2003.

Paik, K.: Global search algorithm for nondispersive flow path extraction, J. Geophys. Res., 113, F04001, doi: 10.1029/2007JF000964, 2008.

Palkovics, W.E. and Petersen, G.W.: Contribution of lateral soil-water movement above a fragipan to streamflow, Soil Sci. Soc. Am. J., 41, 394–400, 1977.

Patrick, W.H. and Henderson, R.E.: Reduction and reoxidation cycles of Manganese and Iron in flooded soil and in water solution, Soil Sci. Soc. Am. J., 45, 855–859, 1981.

Perillo, C.A., Gupta, S.C, and Moncrief, J.F.: Prevalence and initiation of preferential flow paths in a sandy loam with argillic horizon, Geoderma, 89, 307–331, 1999.

Quinn, P.F., Beven, K.J., Chevallier, P., and Planchon, O.: The prediction of hillslope flowpaths for distributed modelling using digital terrain models, Hydrol. Process., 5, 59– 80, 1991.

Reedy, R.C. and Scanlon, B.R.: Soil water content monitoring using electromagnetic induction, J. Geotech. Geoenviron. Eng., 129, 1028–1039, 2003.

Rhoades, J.D., Raats, P.A.C., and Prather, R.S.: Effects of liquid-phase electrical conductivity water content and surface conductivity on bulk soil electrical conductivity, Soil Sci. Soc. Am. J., 40, 651–665, 1976.

Sander, T. and Gerke, H.H.: Preferential flow patterns in paddy fields using a dye tracer, Vadose Zone. J., 6, 105–115, 2007.

Seibert, J. and McGlynn, B.L.: A new triangular multiple flow direction algorithm for computing upslope areas from gridded digital elevation models, Water Resour. Res., 43, W04501, doi:10.1029/2006WR005128, 2007.

Schäuble, H., Marinoni, O., and Hinderer, M.: A GIS-based method to calculate flow accumulation by considering dams and their specific operation time, Comput. Geosci., 34, 635–646, 2008.

Sherlock, M.D. and McDonnell, J.J.: A new too for hillslope hydrologists: spatial distributed groundwater level and soilwater content measured using electromagnetic induction, Hydrol. Process., 17, 1965–1977, 2003.

Sidle, R.C., Noguchi, S., Tsuboyama, Y., and Laursen, K.: A conceptual model of preferential flow systems in forested hillslopes: evidence of self-organization, Hydrol. Process., 15, 1675–1962, 2001.

Soil Survey Division Staff.: Soil Survey Manual, U.S. Department of Agriculture Handbook No. 18, U.S. Government Printing Office, Washington, DC, USA, 1993.

Tarboton, D. G.: A new method for the determination of flow directions and upslope areas in grid digital elevation models, Water Resour. Res., 33, 309–319, 1997.

Thompson, J.A., Pena-Yewtukhiw, E.M., and Grove, J.H.: Soil-landscape modelling across a physiographic region: Topographic patterns and model transportability, Geoderma, 133, 57–70, 2006.

Tsukamoto Y. and Ohta, T.: Runoff process on a steep forested slope, J. Hydrol., 102, 165–178, 1988.

Vachaud, G., De Silans Passerat, A., Balabanis, P., and Vauclin, M.: Temporal stability of spatial measured soil water probability density function, Soil Sci. Soc. Am. J., 49, 822–827, 1985.

Van Genuchten, M.T.: A closed form equation for predicting the hydraulic conductivity of unsaturated soils, Soil Sci. Soc. Am. J., 44, 892–898, 1980.

Formatted: English (U.S.)
Field Code Changed
Formatted: English (U.S.)
Field Code Changed
Formatted: English (U.S.)
Formatted: English (U.S.)

Vogt, J.V., Colombo, R., and Bertolo, F.: Deriving drainage networks and catchment boundaries: a new methodology combining digital elevation data and environmental characteristics, Geomorphology, 53, 281–298, 2003.

Walker, C. and Lin, H.S.: Soil Property Changes after Four Decades of Wastewater Irrigation: A Landscape Perspective, Catena, 73, 63–74, 2008.

Wu, S., Li, J., and Huang, G.H.: A study on DEM-derived primary topographic attributes for hydrologic applications: sensitivity to elevation data resolution, Appl. Geogr., 28, 210–223, 2008.

Yaalon, D.H., Jungreis, C., and Koyumjisky, H.: Distribution and reorganization of manganese in three catenas of Mediterranean soils, Geoderma, 7, 71–78, 1972.

Zhu, Q. and Lin, H.S. Combining sample size, spatial structure, and auxiliary variables to determine optimal kriging in contrasting landscapes, Ecological Modelling, in review, 2009.

Zhu, Q., Lin, H.S., and J. Doolittle Repeated Electromagnetic Induction Surveys for Understanding Landscape Soil and Water Dynamics, Soil Sci. Soc. Am. J. in review, 2009.

Deleted: Interpolation of soil properties based on sample size, spatial structure, and auxiliary variable in two contrasting landscapes

Deleted: Catena

Table 1. Distribution of the number of soil moisture monitoring sites and soil core descriptions among different slope classes, depth to bedrock ranges, and soil series in the study area.

Deleted: at the Kepler Farm

Variable categories		Soil moisture content monitoring sites	Soil matric potential monitoring sites	Soil cores described
Slope (%)	<3	23	11	10
	3~8	80	40	37
	>8	42	23	23
Depth to bedrock (m)	<0.5	34	17	15
	0.5~1.0	59	10	13
	>1.0	52	47	42
Soil series	Opequon	48	27	18
	Hagerstown	63	34	36
	Murrill	17	6	7
	Nolin	10	4	6
	Melvin	7	3	3
Total		**145**	**74**	**70**

Table 2. Methods used to simulate and validate the concentrated subsurface lateral flow paths in the study area. D8: deterministic 8 method single-flow algorithm; RS: relative degree to saturation; EMI: electromagnetic induction; ECa: apparent electrical conductivity.

Interface	Simulation	Validation			
	(D8 algorithm)	Soil hydrologic monitoring		EMI survey	Soil Mn content
1) Ap1–Ap2 2) clay layer 3) soil–bedrock	• Threshold 100 m^2 (relatively wet period) • Threshold 500 m^2 (relatively dry period)	• *RS* values • Temporal stability of *RS* values	• Sites on vs. off the simulated flow paths • Soils at vs. above or below the interface	• Temporal stability of soil ECa values	• Three buffer zones (0–5, 5–10 and 10–15 m) away from the simulated flow paths vs. the rest of study area	• Sites on vs. off the simulated flow paths

Deleted: at the Kepler farm…the …, , …, ... [4]
Formatted Table
Deleted: s
Deleted: al
Deleted: 1)
Deleted: 1)
Formatted ... [5]
Deleted: 1)
Deleted: 1) … ... [6]
Formatted ... [7]
Deleted: 1)
Formatted: English (U.S.)
Formatted: English (U.S.)
Deleted: -
Deleted: 2) t
Formatted ... [8]
Deleted: .
Deleted: 2)
Deleted: 2)
Formatted: English (U.S.)
Deleted: .
Deleted: .

Table 3. The time table of soil water content and matric potential data collections in this study.

Year	2005	2006	2007	2008
Whole area soil water content only (145 sites) – Total 12 times	17 May, 15 June, 10 and 18 July, 3 August, and 14 October	20 and 21 June	13 and 29 March, 20 April, and 15 May	None
Soil water content and matric potential together (76 sites) – Total 14 times	None	20, 21, and 30 June, 3 and 11 July	5 and 29 June, 15 July, 31 October	12, 19, and 26 June, 3 and 10 July

Deleted: at the Kepler Farm

Formatted Table

Deleted: farm

Deleted: along with

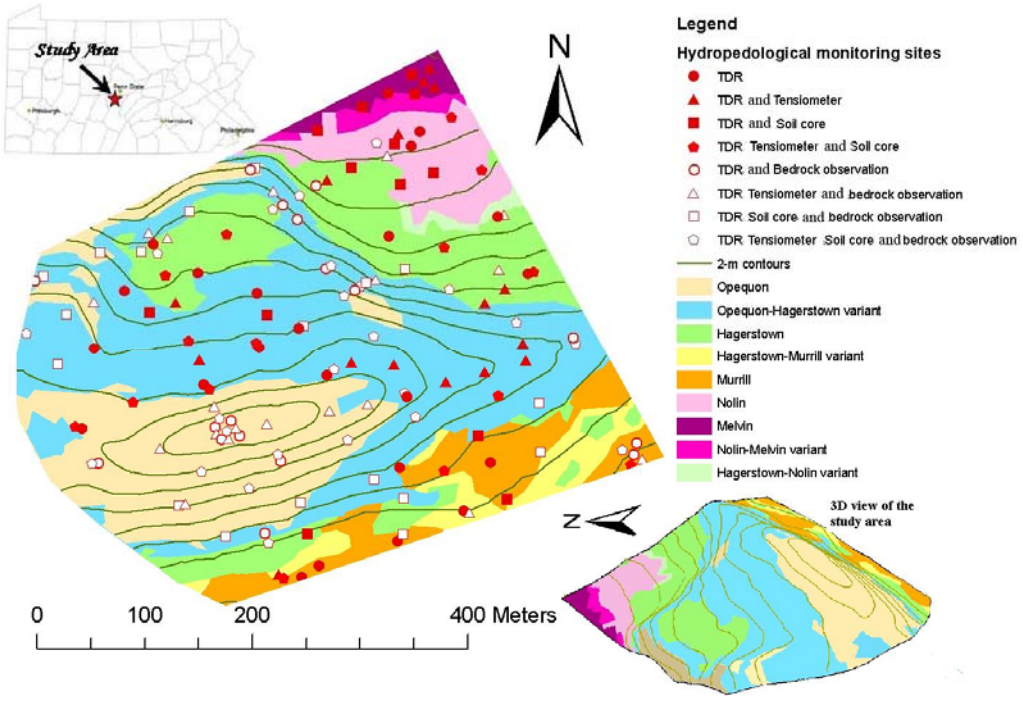

Figure 1. The study area and the spatial distribution of monitoring/observation sites for soil moisture (TDR), matric potential (tensiometers), soil cores, and depth to bedrock (bedrock observation) at the Kepler Farm located in central Pennsylvania, USA. The inset at the lower right corner shows a 3D rendering of the study area. The background map is soil series distribution.

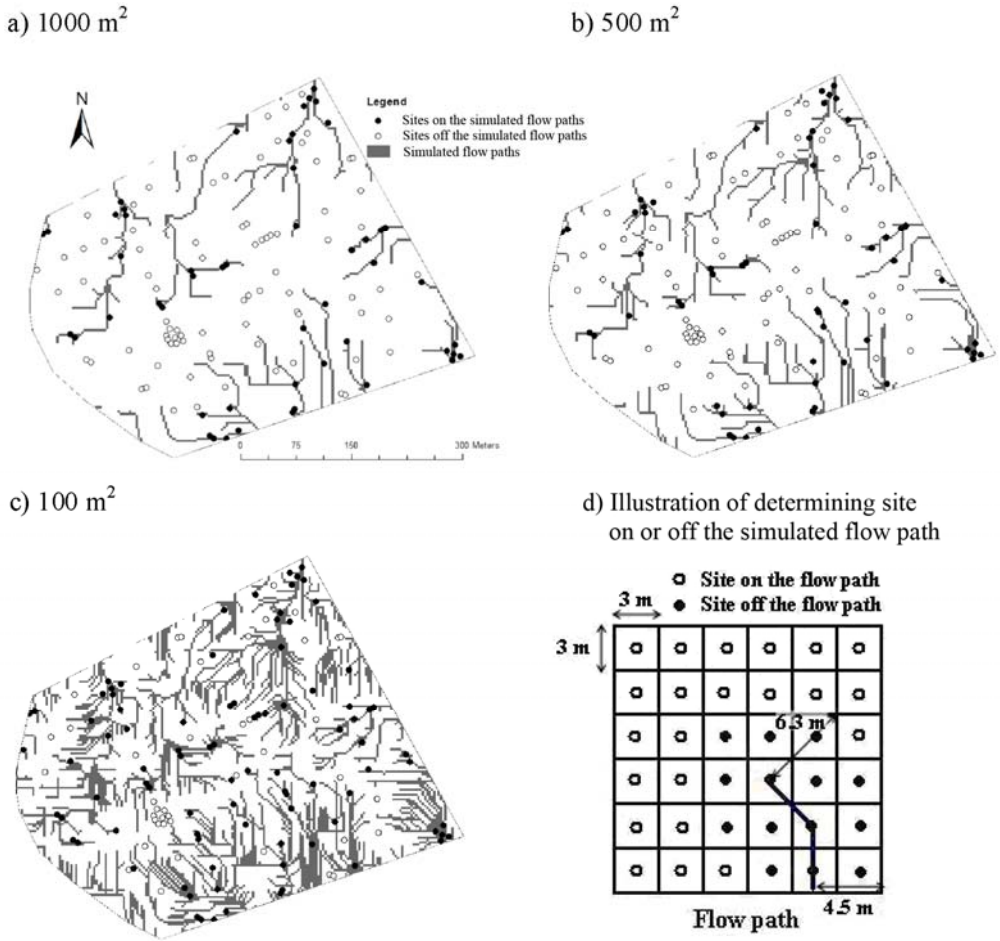

Figure 2. Simulated flow paths at the soil–bedrock interface using three thresholds of contribution area: (a) 1,000 m^2, (b) 500 m^2, and (c) 100 m^2. (d) is an illustration of determining whether a soil moisture monitoring site is on or off the simulated flow path (see the text for details).

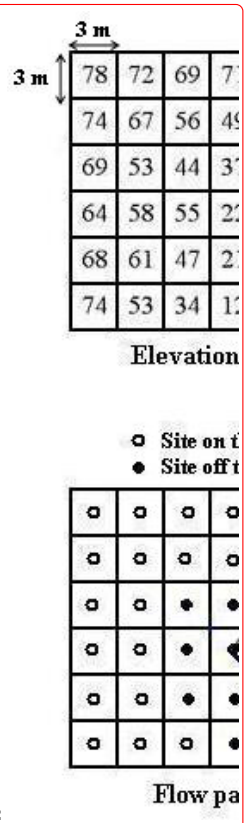

Deleted: ¶

Figure 2. An illustration of determining the flow path from the digital elevation model (DEM) using the deterministic 8 single-flow algorithm (D8). The "direction coding" shows the codes (i.e., 1, 2, 4, 8, 16, 32, 64, and 128) of the eight valid output directions into which flow could travel. The "flow direction" is determined by finding the direction of maximum drop from each cell through the DEM. The "contributing area" of a specific cell is determined by the number of cells draining into it and the cell size ($3\times3=9$ m^2) of the DEM. The "flow path" is generated by setting the threshold of contributing area (e.g., 100 m^2 in the above illustration). If a soil water monitoring site is in a cell of the simulated flow path or adjacent to it, then it is considered as on the simulated flow path in this study.¶

¶

Section Break (Next Page) ... [9]

Deleted: 3

Deleted: and

Deleted: .

Deleted: Simulated flow paths at the Ap1–Ap2 interface and the interface with the clay layer are similar to these shown here.

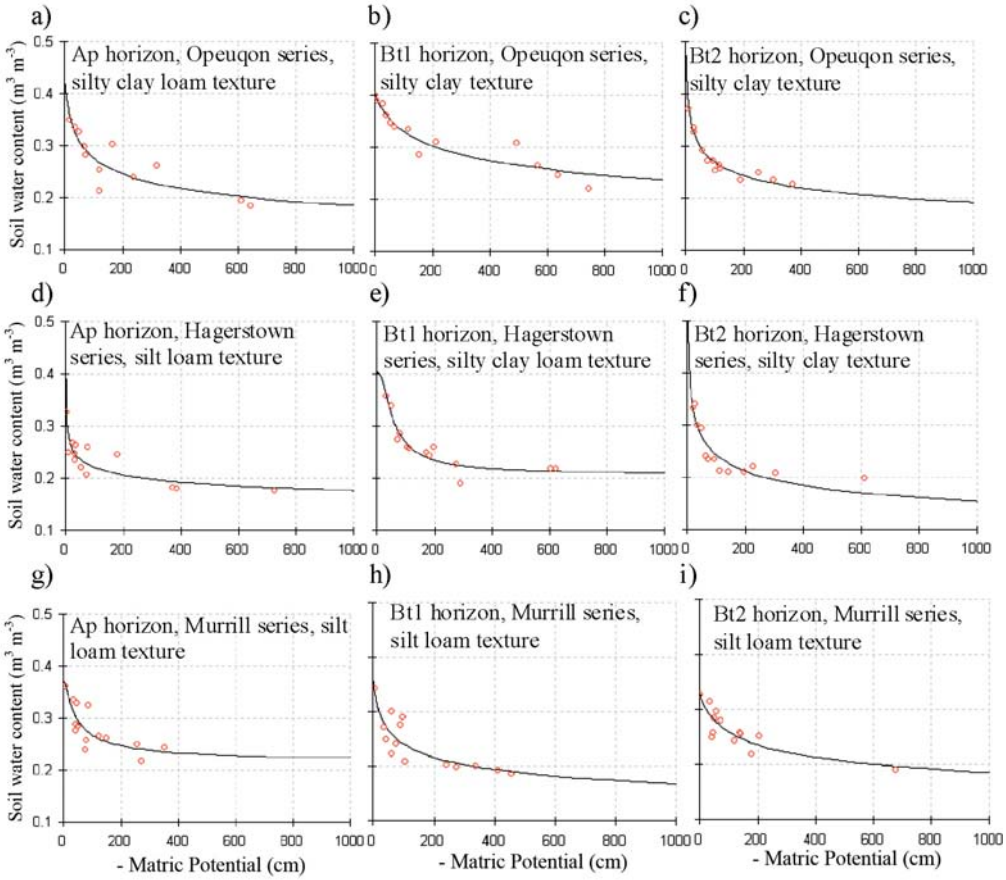

Figure 3. Examples of fitted soil water retention curves using the model of van Genuchten (1980) for (a) Ap (silty clay loam), (b) Bt1 (silty clay), (c) Bt2 (silty clay) horizons of an Opequon series (site #9), (d) Ap (silt loam), (e) Bt1 (silty clay loam), (f) Bt2 (silty clay) horizons of a Hagerstown series (site #85), (g) Ap (silt loam), (h) Bt1 (silt loam), and (i) Bt2 (silt loam) horizons of a Murrill series (site #65).

Deleted: 4

Deleted: at site 9 (the

Deleted: at site 85 (the

Deleted: at site 65 (

Deleted: the

Deleted: using the parametric model of van Genuchten (1980)

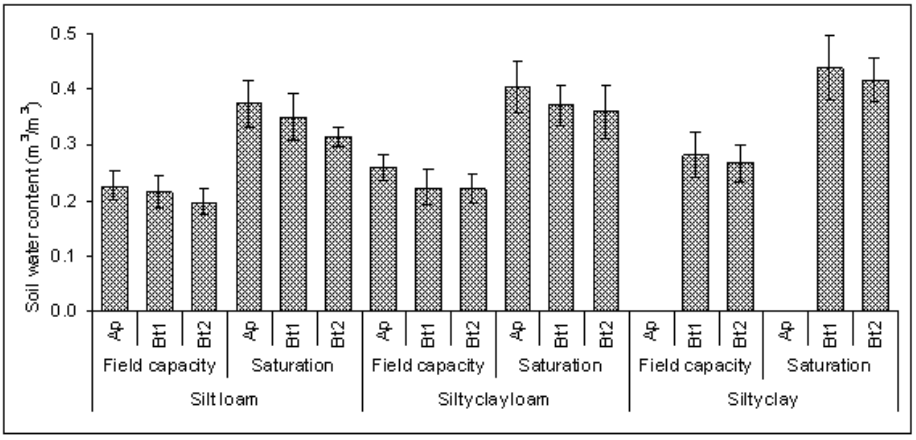

Figure 4. Average volumetric soil water contents and their standard deviations at field capacity and saturation based on field observed soil water content and matrix potential for different textural classes and soil horizons in the study area.

Deleted: 5

Deleted: at the Kepler Farm

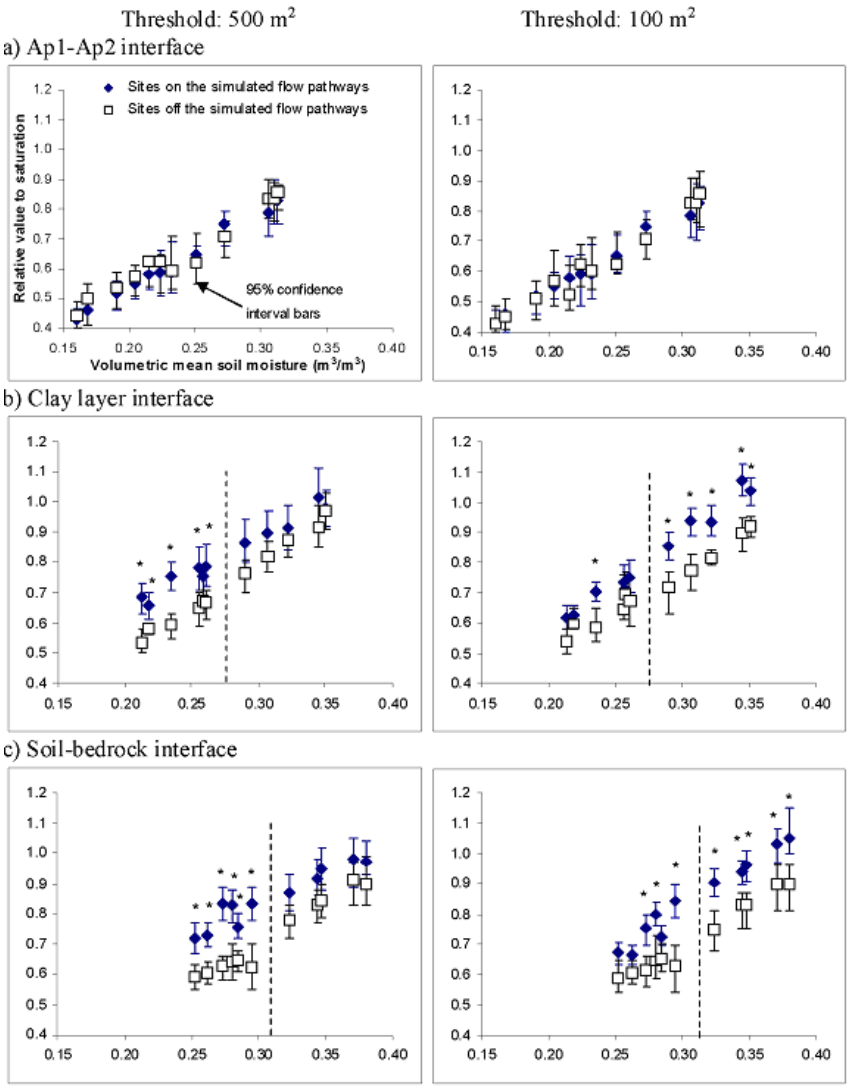

Figure 5. Comparison of the means and 95% confidence intervals of relative saturation (*RS*) at the monitoring sites on and off the simulated flow paths with thresholds of 500 m^2 and 100 m^2 for (a) the Ap1–Ap2 interface, (b) the clay layer interface, and (c) the soil–bedrock interface. Dash lines separate the relatively dry and wet conditions. Bars labeled with asterisks (*) indicate statistically significant difference at $p<0.05$ level between sites on and off the simulated paths.

Deleted: 6

Formatted: English (U.S.)

Formatted: English (U.S.)

Formatted: English (U.S.)

Formatted: English (U.S.)

Formatted: Font: Not Italic, English (U.S.), Superscript

Formatted: English (U.S.)

Formatted: English (U.S.)

Deleted: asteroid

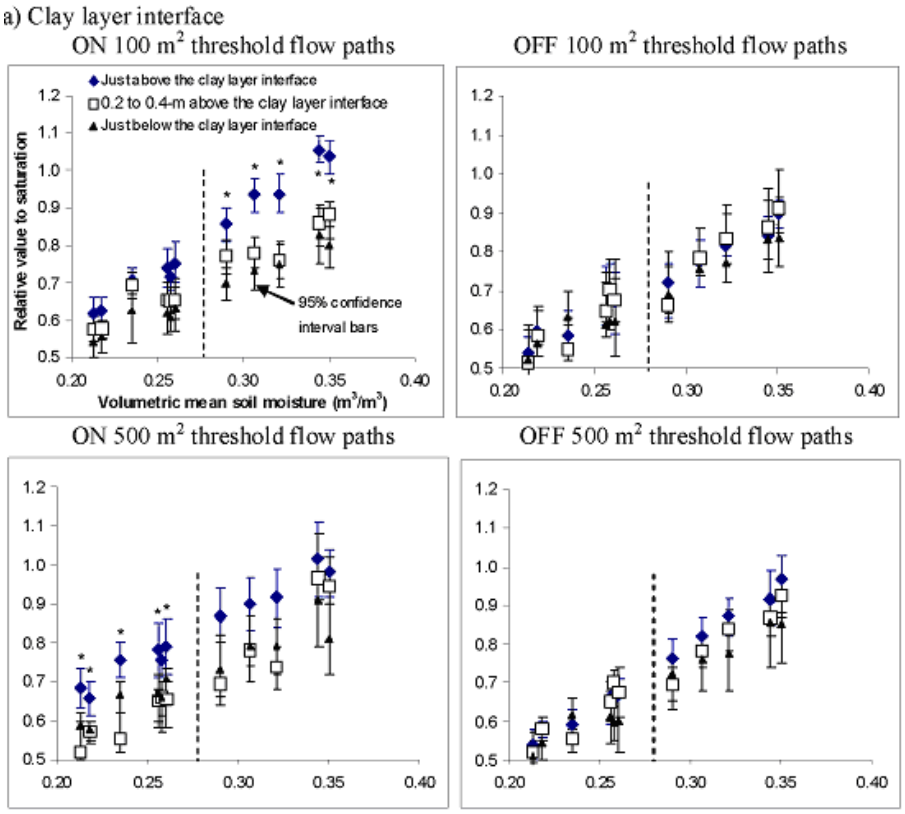

Figure 6. Comparison of the means and 95% confidence intervals of the relative saturation (*RS*) at the monitoring sites on and off the simulated flow paths with thresholds of 500 m^2 and 100 m^2 for (a) the interface with the clay layer and (b) the interface with the bedrock. Within each graph, the comparison is for *RS* just above or below the specified interface and 0.2 m above the interface. Dash lines separate the relatively dry and wet conditions. Bars labeled with asterisks (*) indicate statistically significant difference at $p<0.05$ level.

Deleted: 7

Formatted: Font: Not Italic, Superscript

Deleted: asteroid

Formatted: English (U.S.)

b) Soil-bedrock interface

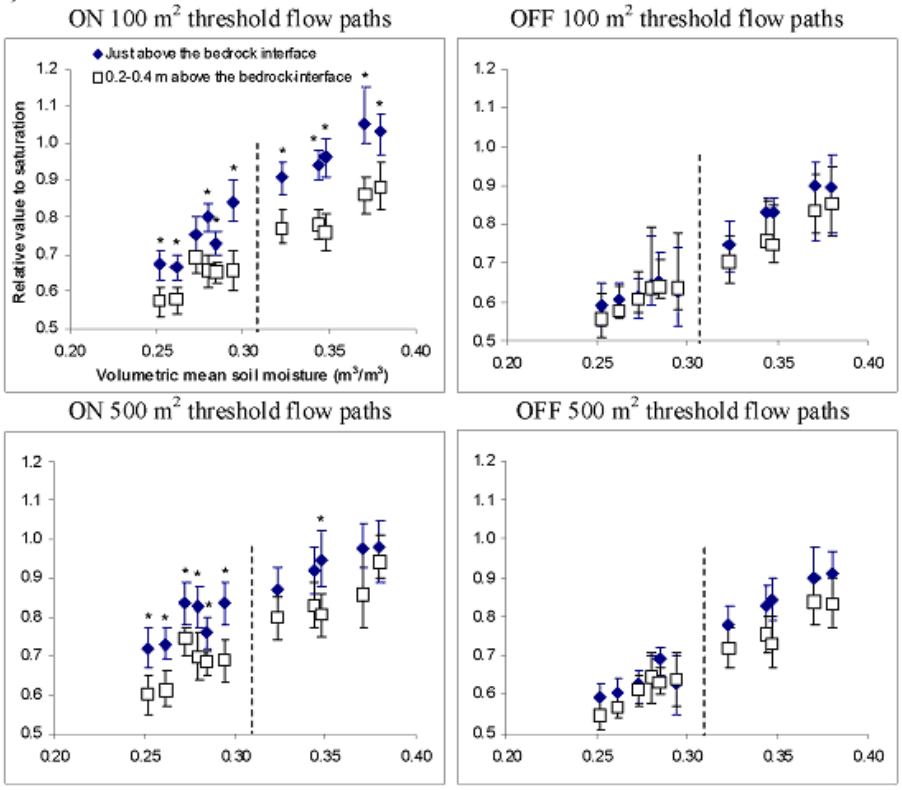

Figure 6. Continued.

Deleted: 7

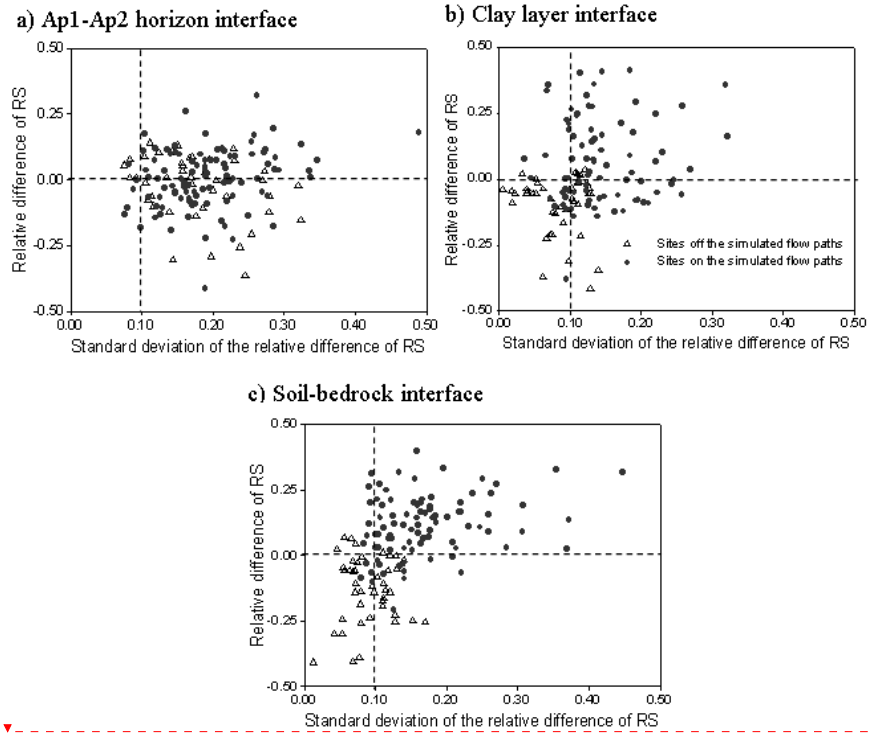

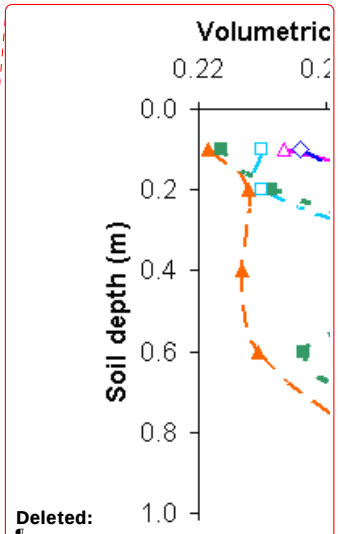

Figure 7. Temporal stability of relative saturation (*RS*) at the monitoring sites on and off the simulated flow paths (using the threshold of 100 m^2) at (a) the Ap1–Ap2 interface, (b) the clay layer interface, and (c) the soil–bedrock interface. Sites with positive relative difference were wetter than the overall average of the entire study area. Sites with high standard deviations of the relative difference were temporally unstable (i.e., more dynamic).

Deleted: ¶

Figure 8. Typical profile distribution of volumetric soil water content in each of the five soil series identified in the study area (i.e., the Opequon, Hagerstown, Murrill, Nolin, and Melvin series).¶

Section Break (Next Page)

Formatted: English (U.S.)

Deleted: 9

Deleted: mean

Deleted: farm

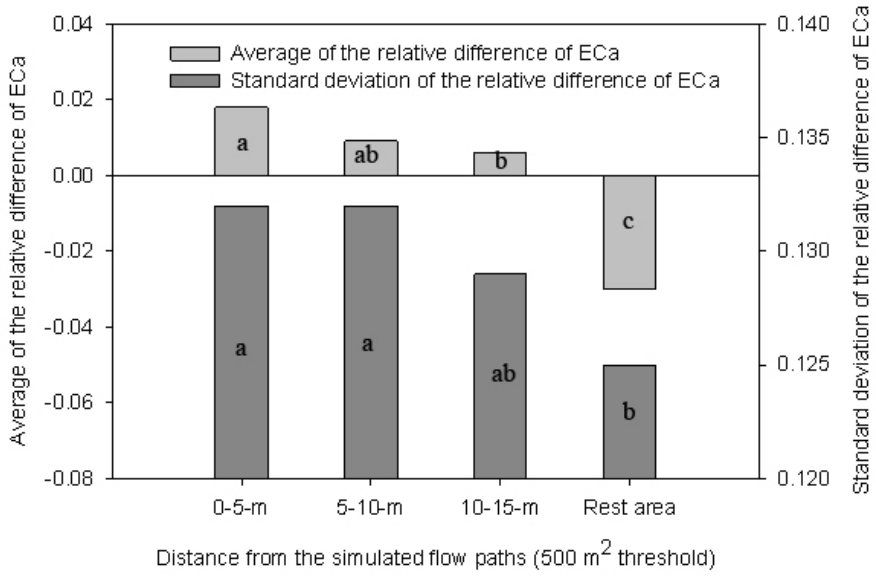

Figure 8. Temporal stability of apparent electrical conductivity (ECa) in areas with different distances away from the simulated flow paths (using the threshold of 500 m^2). Areas with positive relative difference in ECa indicate a higher ECa value than the overall mean of the entire study area. Areas with high standard deviation of the relative difference in ECa indicated temporally more dynamic (or unstable). Bars with the same letter are not statistically significantly different from each other at $p<0.05$ level.

Deleted: 10

Deleted: s

Deleted: s

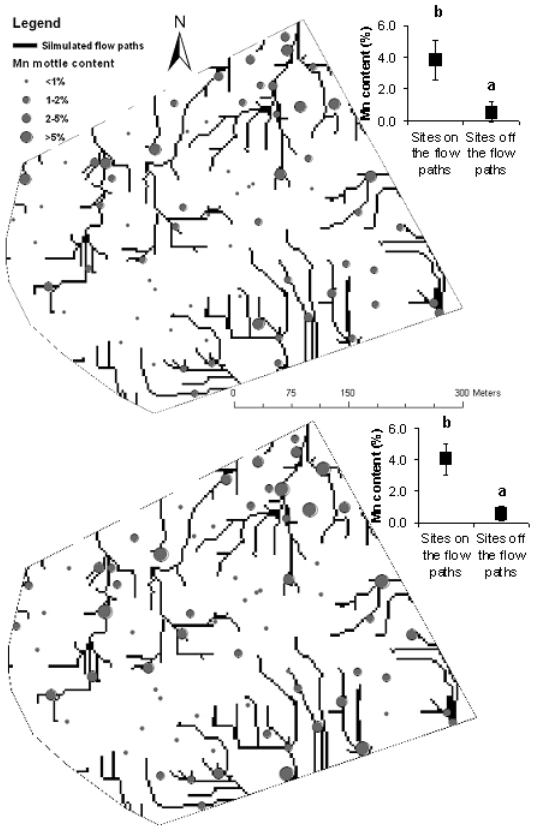

Figure 9. Observed Mn contents in the soil profiles at (a) the clay layer interface and (b) the soil–bedrock interface in relation to the simulated flow paths (using a threshold of 500 m^2). In the insets, Mn contents on and off the simulated flow paths are compared. Bars with different letters are statistically significantly different at $p<0.05$ level.

Deleted: 11

Formatted: English (U.S.)